

สมบัติทางเคมีเชิงกายภาพของแกรไฟีนออกไซด์: การศึกษาเชิงทฤษฎีเด้นซิติฟังก์ชัน

นางสาววิภารัตน์ โหตะรัตน์

วิทยานิพนธ์นี้เป็นส่วนหนึ่งของการศึกษาตามหลักสูตรปริญญาวิทยาศาสตรมหาบัณฑิต

สาขาวิชาเคมี ภาควิชาเคมี

คณะวิทยาศาสตร์ จุฬาลงกรณ์มหาวิทยาลัย

ปีการศึกษา 2555

ลิขสิทธิ์ของจุฬาลงกรณ์มหาวิทยาลัย

บทคัดย่อและแฟ้มข้อมูลฉบับเต็มของวิทยานิพนธ์ตั้งแต่ปีการศึกษา 2554 ที่ให้บริการในคลังปัญญาจุฬาฯ (CUIR)

เป็นแฟ้มข้อมูลของนิสิตเจ้าของวิทยานิพนธ์ที่ส่งผ่านทางบัณฑิตวิทยาลัย

The abstract and full text of theses from the academic year 2011 in Chulalongkorn University Intellectual Repository (CUIR) are the thesis authors' files submitted through the Graduate School.

PHYSICOCHEMICAL PROPERTIES OF GRAPHENE OXIDE: DENSITY
FUNCTIONAL THEORY

Miss Wiparat Hotarat

A Thesis Submitted in Partial Fulfillment of the Requirements
for the Degree of Master of Science Program in Chemistry

Department of Chemistry

Faculty of Science

Chulalongkorn University

Academic Year 2012

Copyright of Chulalongkorn University

Thesis Title PHYSICOCHEMICAL PROPERTIES OF GRAPHENE
 OXIDE: DENSITY FUNCTIONAL THEORY STUDY

By Miss Wiparat Hotarat

Field of study Chemistry

Thesis Advisor Associate Professor Vithaya Ruangpornvisuti, Dr.rer.nat.

Accepted by the Faculty of Science, Chulalongkorn University in Partial
Fulfillment of the Requirements for the Master's Degree

.....Dean of the Faculty of Science
(Professor Supot Hannongbua, Dr.rer.nat.)

THESIS COMMITTEE

.....Chairman
(Assistant Professor Warinthorn Chavasiri, Ph.D.)

.....Thesis Advisor
(Associate Professor Vithaya Ruangpornvisuti, Dr.rer.nat.)

.....Examiner
(Kanet Wongravee, Ph.D.)

.....External Examiner
(Assistant Professor Khajadpai Thipyapong, Ph.D.)

วิภารัตน์ โหตะรัตน์: สมบัติทางเคมีเชิงกายภาพของแกรฟีนออกไซด์: การศึกษาเชิงทฤษฎีเคมียุติฟังก์ชัน (PHYSICOCHEMICAL PROPERTIES OF GRAPHENE OXIDE: DENSITY FUNCTIONAL THEORY) อ. ที่ปรึกษาวิทยานิพนธ์หลัก: รศ. ดร.วิทยา เรืองพรวิสุทธิ, 53 หน้า.

ศึกษาปฏิกิริยาออกซิเดชันของแกรฟีน (graphene) โดยใช้โมเลกุลของออกซิเจน (O_2) และไฮโดรเจนเปอร์ออกไซด์ (H_2O_2) เพื่อให้เกิดเป็นแกรฟีนออกไซด์ (GO) ด้วยวิธีเคมียุติฟังก์ชัน (DFT) โดยศึกษาโครงสร้างที่เหมาะสมของการเกิดออกไซด์ ไฮดรอกซิล คาร์บอนิล และคาร์บอกซิลแกรฟีนออกไซด์ ศึกษาการดูดซับออกซิเจนและไฮโดรเจนเปอร์ออกไซด์บนแผ่นแกรฟีนชนิดสมบูรณ์ (Pristine graphene) และชนิดบกพร่องแบบสโตนเวลล์ (Stone-wales defect) และศึกษาพลังงานปฏิกิริยาออกซิเดชันของแกรฟีนโดยโมเลกุลของออกซิเจนในการเกิดคาร์บอนิลแกรฟีนออกไซด์และก้ำซมีเทน และการศึกษาแบบจำลองของการดูดซับของออกซิเจนสามโมเลกุล ($3O_2$) และไฮโดรเจนเปอร์ออกไซด์สามโมเลกุล ($3H_2O_2$) เมื่อเกิดการดูดซับแบบกลุ่มบนแผ่นแกรฟีนชนิดสมบูรณ์และชนิดบกพร่องแบบสโตนเวลล์

ภาควิชา.....เคมี.....ลายมือชื่อนิสิต.....
 สาขาวิชา.....เคมี.....ลายมือชื่อ อ.ที่ปรึกษาวิทยานิพนธ์หลัก.....
 ปีการศึกษา.....2555.....

5472102023: MAJOR CHEMISTRY

KEYWORDS: GRAPHENE OXIDE; EPOXY AND HYDROXYL; CARBONYL AND CARBOXYL; DFT

WIPARAT HOTARAT: PHYSICOCHEMICAL PROPERTIES OF GRAPHENE OXIDE: DENSITY FUNCTIONAL THEORY STUDY. ADVISOR: ASSOC. PROF. VITHAYA RUANGPORNVISUTI, Dr.rer.nat. , 53 pp.

Oxidation of graphene by oxygen and hydrogen peroxide molecule to afford graphene oxide (GO) has been studied by density functional theory (DFT) method. Formation of epoxy, hydroxyl, carbonyl carboxyl GOs and their optimized structures has been investigated. Adsorption of oxygen and hydrogen peroxide molecules on pristine and SW-defective GOs were investigated. The reaction energies for oxidation of graphene by oxygen molecule to afford carbonyl GO and hydrogen molecule and oxidation hydrogenation of graphene by hydrogen molecule to afford carboxyl GO and methane molecule were obtained. GOs simulated by random adsorptions of $3\text{H}_2\text{O}_2$ and 3O_2 on basal planes of one and both sides of pristine and SW-defective graphene sheets were examined.

Department: Chemistry..... Student's Signature

Field of Study: Chemistry..... Advisor's Signature

Academic Year: 2012.....

ACKNOWLEDGEMENTS

This study was carried out at the Chemistry Department, Faculty of Science, Chulalongkorn University. I wish to express sincere thanks to my advisor Associate Professor Dr. Vithaya Ruangpornvisuti for providing me all necessary facility. I am most appreciative for his teaching and advice for my research. I would not have accomplished this far and this thesis would not have been completed without all the support and advice that I have always received from him throughout the course of this research.

I would like to really thank Assist. Prof. Dr. Warinthorn Chavasiri, Dr. Kanet Wongravee and Assist. Prof. Dr. Khajadpai Thipyapong for kind suggestion on my thesis committee. Their sincere suggestions are definitely imperative for accomplishing my thesis.

I take opportunity to thank all members of the research groups for their help and suggestion.

Finally, I would like to thank my parent for always supporting and trusting all of time of this reseach.

CONTENTS

	Page
ABSTRACT IN THAI	iv
ABSTRACT IN ENGLISH	v
ACKNOWLEDGEMENTS	vi
CONTENTS	vii
LIST OF TABLES	ix
LIST OF FIGURES	x
LIST OF ABBREVIATIONS	xiii
CHAPTER I INTRODUCTION	1
1.1 Background.....	1
1.2 Fundamentals of the graphene oxide structure.....	2
1.3 Literature reviews	5
1.4 Objective.....	6
CHAPTER II THEORETICAL BACKGROUND	8
2.1 The Schrödinger equations.....	8
2.2 HF Approximation.....	9
2.3 DFT method.....	11
2.3.1 The Kohn–Sham energy and the Kohn–Sham equations.....	12
2.3.1.1 The Kohn–Sham energy.....	12
2.3.1.2 The Kohn–Sham equations.....	15
2.4 Gaussian basis sets.....	16
2.4.1 Linear Combination of Atomic Orbitals.....	16
2.4.2 Minimal basis sets.....	17
2.4.3 Split–valence basis sets.....	17
2.4.4 Polarized basis sets.....	18

	Page
2.4.5 Basis sets incorporating diffuse functions.....	18
2.5 The Potential Energy Surface.....	18
CHAPTER III DETAILS OF THE CALCULATIONS.....	20
3.1 Computational method.....	20
3.2 Cluster models.....	21
3.3 Definition of oxidation for producing GO.....	23
3.4 PES scans for di-hydroxyl GO.....	23
3.5 Notations for GOs.....	24
CHAPTER IV RESULTS AND DISCUSSION.....	25
4.1 Conformations for epoxy GO.....	25
4.2 Conformations for hydroxyl GO.....	29
4.3 Formations for carbonyl and carboxyl GOs.....	36
4.4 GO simulation for adsorption of 3H ₂ O and 3O ₂ on graphene.....	37
CHAPTER V CONCLUSIONS.....	39
5.1 Conclusions.....	40
REFERENCES.....	41
APPENDIX.....	47
VITAE.....	53

LIST OF TABLES

Table	Page
4.1 Relative energies of configurations of di-epoxy GOs compared with lowest energies for each cluster models, their frontier orbital energies and energy gaps.....	27
4.2 Adsorption energies of oxygen molecule on the graphene basal plane to afford epoxy GOs and strain energies of their graphene sheets.....	29
4.3 Relative energies of configurations of di-hydroxyl GOs compared with lowest energies for each cluster models, their frontier orbital energies and energy gaps.....	31
4.4 Adsorption energies of hydrogen peroxide molecule onto the graphene basal plane to afford hydroxyl GOs and strain energies of their graphene sheets.....	33
4.5 Reaction energies for oxidation processes of graphene sheets at their edges to afford carbonyl and carboxyl GOs.....	37
4.6 GO simulations for random adsorptions of 3H ₂ O ₂ and 3O ₂ on basal planes of one and both sides of pristine and SW-defective graphene sheets	38

LIST OF FIGURES

Figure		Page
1.1	The structural models of graphene oxide: (a) Hofmann, (b) Ruess, (c) Scholz–Boehm and Nakajima–Mutsuo.....	4
1.2	Structural of graphene oxide in Lerf and Klinowski model.....	4
3.1	Cluster models for (a) pristine graphene, Model 1 or GM1 (C ₅₄ in C ₉₆ H ₂₄ cluster), (b) pristine graphene, Model 2 or GM2 (C ₄₂ in C ₈₀ H ₂₂ cluster), (c) SW–defective graphene, Model 3 or GM3 (C ₄₂ in C ₈₀ H ₂₂ cluster), (d) Model 4 and (e) Model 5. Ball atoms are defined as flexible atoms treated in optimization; the rest atoms are frozen. C–C bonds labeling is used in di–epoxide GOs notation.....	22
4.1	Configurations of di–epoxide in vicinity of pristine graphene sheets center, noted as (a) O ¹ O ³ /GM1, (b) O ¹ <u>Q</u> ³ /GM1, (c) O ^{1*} <u>Q</u> ¹ /GM1, (d) O ¹ <u>Q</u> ³ /GM1, (e) O ^{1*} <u>Q</u> ² /GM1 and (f) O ¹ <u>Q</u> ³ /GM1. Their relative energies and bond lengths are in kcal/mol and Å, respectively.....	26
4.2	Configurations of di–epoxides in vicinity of SW–defective graphene sheets noted (a) O ² O ² /GM3, (b) O ² O ³ /GM3, (c) O ¹ O ³ /GM3, (d) O ¹ O ⁵ /GM3, (e) O ⁶ O ² /GM3, (f) O ² O ³ /GM3, (g) O ² <u>Q</u> ² /GM3, (h) O ⁶ <u>Q</u> ⁵ /GM3, (i) O ¹ <u>Q</u> ³ /GM3, (j) O ¹ <u>Q</u> ⁵ /GM3, (k) O ⁶ <u>Q</u> ³ /GM3 and (l) O ⁶ <u>Q</u> ⁵ /GM3. Their relative energies and bond lengths are in kcal/mol and Å, respectively.....	28
4.3	Configurations of di–hydroxide on pristine graphene sheets, noted as (a) (OH) ₂ (1)/GM2, (b) (OH) ₂ (2)/GM2, (c) (OH) ₂ (3)/GM2, (d) (OH) ₂ (4)/GM2, (e) (OH) ₂ (5)/GM2, (f) (OH) ₂ (6)/GM2, (g) (OH) ₂ (7)/GM2, (h) (OH) ₂ (8)/GM2, (i) (OH) ₂ (9)/GM2 and (j) (OH) ₂ (10)/GM2 Their relative energies and bond lengths are in kcal/mol and Å, respectively.....	30

- 4.4 Configurations of di-hydroxide in vicinity of SW-defective graphene sheets, noted as (a) $(\text{OH})_2(1)/\text{GM3}$ (b) $(\text{OH})_2(2)/\text{GM3}$, (c) $(\text{OH})_2(3)/\text{GM3}$, (d) $(\text{OH})_2(4)/\text{GM3}$, (e) $(\text{OH})_2(5)/\text{GM3}$, (f) $(\text{OH})_2(6)/\text{GM3}$, (g) $(\text{OH})_2(7)/\text{GM3}$, (h) $(\text{OH})_2(8)/\text{GM3}$, (i) $(\text{OH})_2(9)/\text{GM3}$, (j) $(\text{OH})_2(10)/\text{GM3}$, (k) $(\text{OH})_2(11)/\text{GM3}$, (l) $(\text{OH})_2(12)/\text{GM3}$, (m) $(\text{OH})_2(13)/\text{GM3}$, (n) $(\text{OH})_2(14)/\text{GM3}$, (o) $(\text{OH})_2(15)/\text{GM3}$, (p) $(\text{OH})_2(16)/\text{GM3}$ and (q) $(\text{OH})_2(17)/\text{GM3}$. Their relative energies and bond lengths are in kcal/mol and Å, respectively. Their relative energies and bond lengths are in kcal/mol and Å, respectively..... 34
- 4.5 Configurations of di-hydroxide in vicinity of SW-defective graphene sheets, noted as (a) $(\text{OH})_2(18)/\text{GM3}$, (b) $(\text{OH})_2(19)/\text{GM3}$, (c) $(\text{OH})_2(20)/\text{GM3}$, (d) $(\text{OH})_2(21)/\text{GM3}$, (e) $(\text{OH})_2(22)/\text{GM3}$, (f) $(\text{OH})_2(23)/\text{GM3}$, (g) $(\text{OH})_2(24)/\text{GM3}$, (h) $(\text{OH})_2(25)/\text{GM3}$, (i) $(\text{OH})_2(26)/\text{GM3}$, (j) $(\text{OH})_2(27)/\text{GM3}$, (k) $(\text{OH})_2(28)/\text{GM3}$, (l) $(\text{OH})_2(29)/\text{GM3}$, (m) $(\text{OH})_2(30)/\text{GM3}$, (n) $(\text{OH})_2(31)/\text{GM3}$, (o) $(\text{OH})_2(32)/\text{GM3}$, (p) $(\text{OH})_2(33)/\text{GM3}$ and (q) $(\text{OH})_2(34)/\text{GM3}$. Their relative energies and bond lengths are in kcal/mol and Å, respectively. Their relative energies and bond lengths are in kcal/mol and Å, respectively..... 35
- 4.6 Optimized structures of carbonyl GOs of which oxygen atoms bonded to C atoms at (a) armchair edge, (b) at zigzag edge connection with armchair edge, (c) at middle zigzag edge and (d) carboxyl GO afforded due to carbon atom at armchair edge. Ball shaped atoms were treated as flexible atoms employed in structure optimizations. All the reaction energies (kcal/mol) for GOs are computed based on graphene Model 4, except reaction in (c) based on Model 5..... 36

4.7	Optimized structures of GOs as random adsorptions of $3\text{O}_2+3\text{H}_2\text{O}_2$ on (a) one side, (b) both sides of pristine graphene sheets, (c) one side and (d) both sides of SW-defective graphene sheets. For adsorption on both sides, $\text{O}_2+2\text{H}_2\text{O}_2$ and $2\text{O}_2+\text{H}_2\text{O}_2$ are adsorbed on up and down sides, respectively. Top and side views are located at top and bottom, respectively.....	37
-----	---	----

LIST OF ABBREVIATIONS

ADF	Annular dark file
AFM	Atomic force microscopy
AM1	Austin model 1
AO	Atomic orbital
B3LYP	Beck 3 Lee–Yang–Parr
DFT	Density functional theory
E	Energy
EELS	Electron energy loss spectrophotometry
GO	Graphene oxide
\hat{H}	Hamiltonian operator
HF	Hartree–Fock
LCAO	Linear combination of atomic orbitals
MD	Molecular dynamic
NEB	Nudge elastic band
NMR	Nuclear magnetic resonance
PES	Potential energy surface
SCF	Self-consistent field
STO	Slater type orbital
SW	Stone–Wales
VASP	Vienna ab initio simulation package
Å	Angstrom
\hat{f}	Fock operator
ψ	Wave function
ϕ	Basis functions
ρ	Electron density
Φ	Spatial orbital
ζ	Effective nuclear charge
χ	Electron wave function

CHAPTER I

INTRODUCTION

1.1 Background

The graphite oxide sheet or graphene oxide (GO) has demonstrated its potential for many applications, such as functional materials [1,2], electronic devices [3–5], chemical catalysts [6–10], gases storages [11–14] and artificial receptors [15]. GO was prepared by oxidation of graphite with a water-free mixture of concentrated sulfuric acid, sodium nitrate and potassium permanganate [16] and newly prepared and characterized by modern method [1]. The local structure of GO was studied by density functional theory method and GO was defined as the partially oxidized graphene which is linked by peroxide-like linkages [17]. The presence of epoxy groups and double bonds of GO and its derivatives was found by solid-state C-NMR spectroscopic method [18]. GO was reviewed including its synthesis, structure and reactions which are reductions as removing oxygen groups from graphene oxide and chemical functionalizations as adding other chemical functionalities to GO [19]. Due to possible structures of GO are somewhat variety, its structural models were proposed by many research groups, namely by Hofmann and Holst [20], Ruess [21], Scholz and Boehm [22] and Nakajima and Matsuo [23] from experiments. The GO models were theoretically constructed and asserted by comparing energies [24–28].

Synthesis, properties and applications of GO and GO-derived graphene-based materials were reviewed [29]. The atomic level structure and mechanical properties of GO paper-like materials were elucidated by molecular dynamics simulations and the individual GO platelets interlinked via a non-uniform network of hydrogen bonds mediate by oxygen-containing functional groups and water molecules were found [30]. Since oxygen functionalities existing in GO have been identified, epoxide ($-O-$) and hydroxyl ($-OH$) located on the basal plane of GO but carbonyl ($-C=O$) and carboxyl ($-COOH$) distributed at the edges of GO were observed [31–40]. Adsorption

configurations of hydroxyl and epoxy groups on and pristine and defective graphene and co-existing in GO were studied [41]. For carbon to oxygen ratios in GO lying between 2.1 to 2.9 [16] and 2.9 [42] were found. Ratios for oxygen-containing groups, epoxide: hydroxyl: carbonyl/carboxyl of 4.9: 19.3: 11.15 have been also reported [42].

1.2 Fundamentals of the GO structures

GO is two-dimensional hexagonal plane in which are held together by sp^2 - and sp^3 -hybridization whose structures were characterized by X-rays and NMR techniques [18, 33]. The structures model of GO have been proposed by many research groups such as Hofmann, Ruess, Scholz-Boehm, Nakagima-Matsuo and Lorf-Klinowski models. Hofmann model was proposed by Hofmann and Holst that structure of GO consists of epoxide groups on the basal plane of graphene [21], Ruess model was proposed by Ruess that structure of GO consists of epoxide groups in the position 1,3 and hydroxyl groups in the position 4 of cyclohexane. These model were shown sp^3 -hybridized system than sp^2 -hybridized of basal plane [21]. Scholz-Boehm model was suggested by Scholz and Boehm that GO model consists of quinoidal species in backbone [22]. Nakagima-Matsuo model was proposed by Nakagima and Matsuo that structure of GO consists of O^- species and hydroxide groups on basal plane [23].

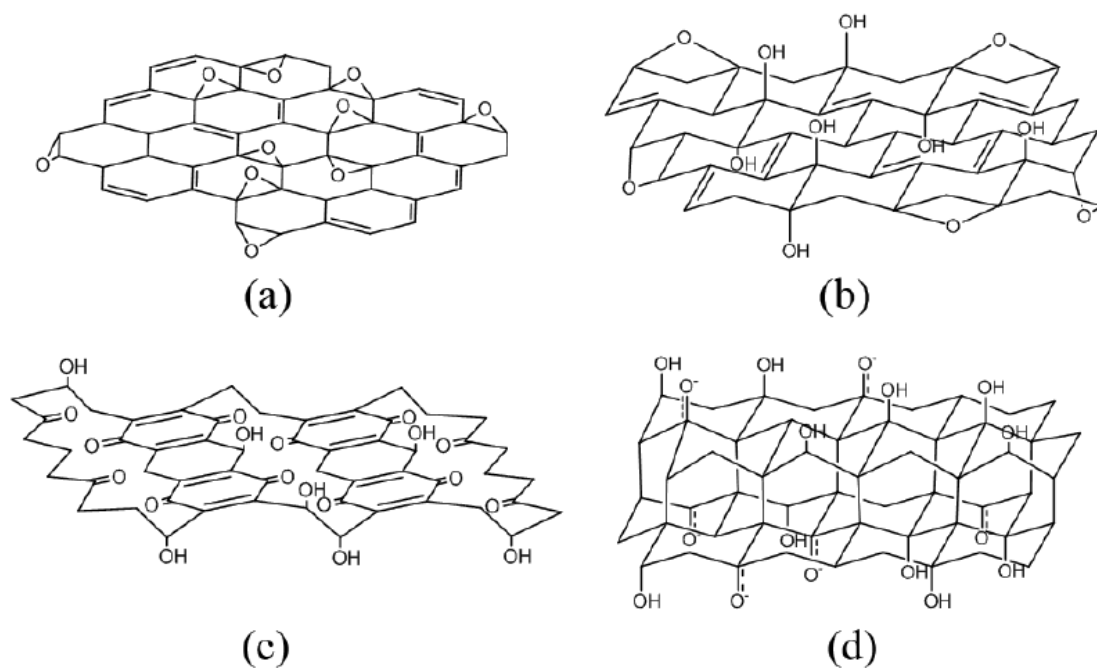


Figure 1.1 The structural models of GO: (a) Hofmann, (b) Ruess (c) Scholz-Boehm and (d) Nakajima-Matsuo.

The most popular model is Lerf–Klinowski model. This GO model was studied by Lerf and Klinowski by using solid state nuclear magnetic resonance (NMR) spectroscopy and X-rays techniques. Lerf–Klinowski model consists of epoxide and hydroxide groups on basal plane, carboxyl groups attached at edge of graphene [18, 35].

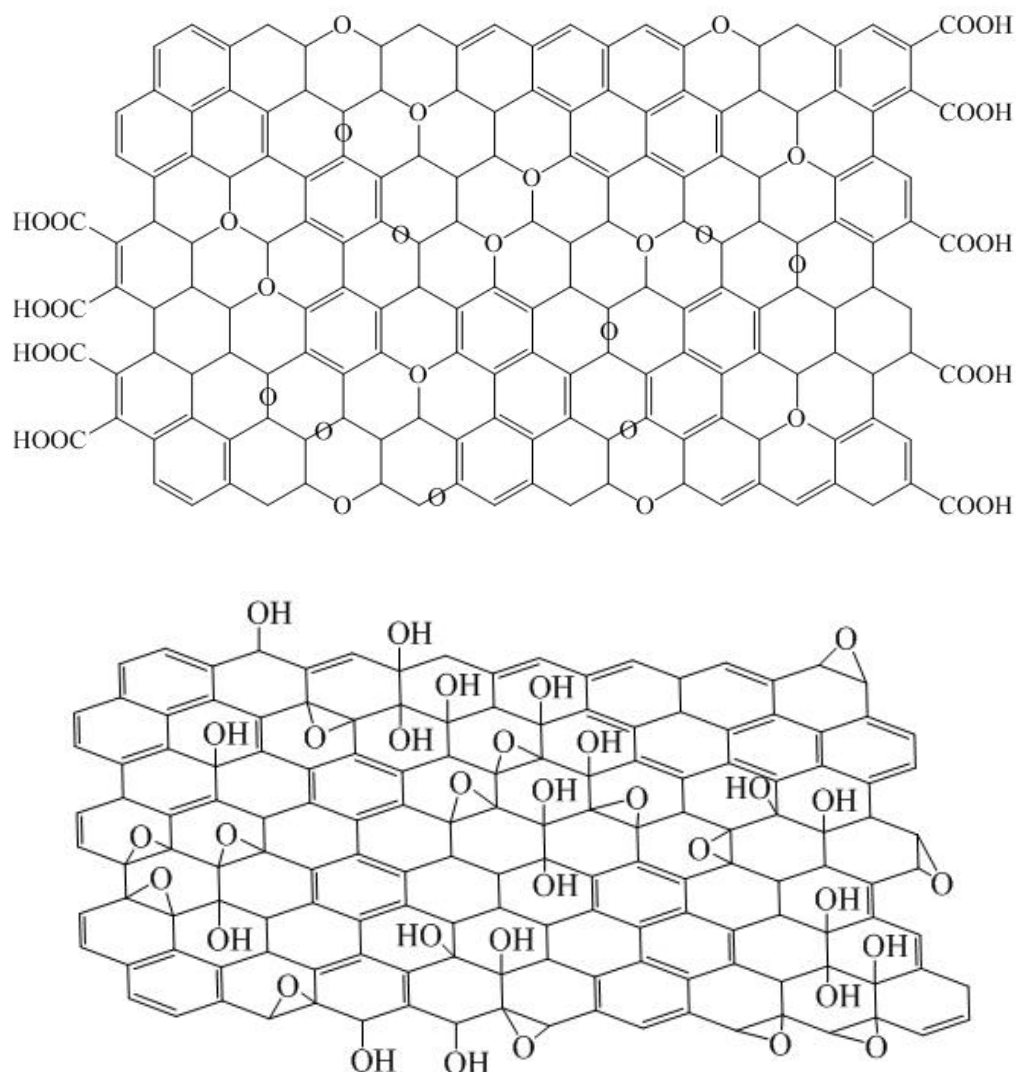


Figure 1.2 Structures of GO in the Lerf and Klinowski model.

The experimental data show that C:O atomic ratio of GO depends on synthesis techniques as well as length of reaction [38, 43]. Chemical oxidation of graphite causes breaking up sp^2 -hybridization to generate defect GO structure and increasing distance between layer of graphite oxide from 3.35 Å to 6.8 Å [44]. Functionalization of graphene with oxygen-containing group derives hydrophilicity on surface of GO. GO can be dispersed in water and other organic solvents [45], the bond length between two carbon atoms increases from 1.407 Å of graphene to 1.514 Å and adsorption energy is -3.14 eV [46]. GO structure is shown high chemical reactivity and large specific surface area which can be modified on several techniques.

1.3 Literature reviews

In 2011, Zhang and Zhang [47] studied on the topics of directly exfoliate of graphite oxide to GO nanosheets without ultrasonication. Aqueous colloid of graphite oxide is precursor for exfoliation. They used a modified Hummers method to prepare aqueous colloids of graphite oxide in de-ionized water with stir and heat. After 3-days centrifuged solution to remove unexfoliate GO and yield turn to be dark brow with little sediments. The results from exfoliation were characterized by atomic force microscopy (AFM). GO sheets was shown thickness of sheets in range from 0.8 to 2.0 nm. GO layer revealed oxygen-containing groups on sheets such as C=O (1718 cm^{-1}), OH (3240 cm^{-1}), C-O (1047 cm^{-1}) and C-OH (1223 cm^{-1}). The Van der Waals interaction between GO layers in graphite oxide sheets makes it high strong hydrophilicity and easy to disperse in water.

In 2009, Mkhukan and *et al.* [46] studied on the topic of atomic and electronic structure of GO. The atomic and electronic of GO were studied by using annular dark file (ADF). ADF was used to detect image of single and multilayer sheets. The structure of GO was measured by using electron energy loss spectrophotometry (EELS) and scanning transmission microscope (STEM). The investigation of GO reveals that GO structure is predominantly amorphous because distortion from sp^3 C-O bond about 40% and O:C ratio as 1:5. The results from AFM reveal that the thickness of monolayer is 1.6 nm and ration due to mono-, bi- and tri-layer scale as 1:1.6:2.2. ADF was shown the thickness ratio of mono-, bi-, and tri-layer as 1.0:1.5:2.0 as same as results from AFM. These results were explained by effectively packing of GO layer which the oxygen groups were attached on both side of graphene sheet and form randomly covalent bond with carbon atom. Oxygen attached on surface created defect sheet of GO. The electronic structure of GO sheet was studied on C and O K-edge by EELS and found that GO is both of sp^2 - and sp^3 -hybridization presented on GO sheet.

In 2011, Lu and *et al* [48] studied on structure of GO in terms of thermodynamic and kinetics by using computational calculations i.e. DFT, molecular

dynamic (MD) simulations and the veinna ab initio simulation package (VASP). The optimization structure of GO was shown that the bond length of C–O is 1.46 Å and distance between two oxidized carbon atom is 1.51 Å and O–H bond length is 1.49 Å. The results from thermodynamics calculations reveal that sovation energy (ΔG_{sol}) is -0.08 eV for isolated epoxide group while isolated hydroxyl group ΔG_{sol} is -0.25 eV. The kinetics properties of the isolated hydroxyl group reveal that energy barrier is 0.27 eV and the distance between C–O in initial state is 1.51 Å and in the transition state is 2.51 Å. The calculation of diffusion barrier for isolated epoxy group is 0.74 eV.

In 2010, Ghaderi and Peressi [41] studied on the adsorption of hydroxyl functional groups on pristine graphene and defected graphene based on numerical method. The adsorption energy of individual OH on the top of carbon atoms is -0.54 eV. The nudge elastic method (NEB) was used to explain OH diffusion in graphene sheets. The results from NEB method revealed that OH can diffused on graphene surface with energy barrier 0.32 eV. OH groups can adsorbed on the both side of graphene. The adsorption energy for one–side is -1.10 eV per molecule, energy gain 1.12 eV per pair and two–side is -1.29 eV per molecule, energy gain is 1.50 eV per pair. The formation energy of OH groups on stone–wales (SW) defect is 5.20 eV within range from 4.8 to 10.4 eV in previous work. The adsorption energy of OH adsorbed on SW defect is -1.80 eV and energy barrier for diffusion is 1.39 eV. OH pair binds to on one–side SW with adsorption energy -1.8 eV/OH and -2.23 eV/OH for two–side adsorption.

1.4 Objective

In this study, all possible functionalized structures for epoxide and hydroxyl groups on basal plane of graphene, on the other hand carbonyl and carboxyl groups was added to edge of graphene. The functionalization of graphene cluster model with oxygen–containing groups such as hydroxyl (–OH), epoxide (–O–), carbonyl (–C=O) and carboxyl (–COOH) groups was investigated using the quantum chemical calculations based on the DFT method. Cluster models containing $C_{80}H_{22}$ model and

$C_{96}H_{24}$ model. Adsorption energy and electronic properties of functionalization were obtained by the calculation at the B3LYP/6–31(d,p) level. The structure of double hydroxide was studied by PES scan by using AM1 method. Due to carbonyl and carboxyl GOs, carbon atoms of these two functional groups have been changed from their graphene sheet during oxidation processes and their structures have been obtained. Reaction energies of oxidation process to afford carbonyl and carboxyl GOs have been determined.

CHAPTER II

THEORETICAL BACKGROUND

The fundamental of quantum chemistry was studied under the Schrödinger equation [49–51]. The main of quantum chemistry based on approximate solutions of the Schrödinger equation relate to ground state energy of individual atoms and molecules, excited states and transition state via chemical reactions. The computational quantum chemistry was separated into division of semi-empirical, Hartree-Fock (HF) and density functional theory (DFT) that can be used to calculation and prediction of electronics properties, molecular structure, bond strength and other characteristics of chemical bonds.

2.1 The Schrödinger equations

The first principle of quantum chemistry is the Schrödinger equations [52, 53] that use to be approximate of ground state energy of electron in molecule

$$\hat{H}\Psi = E\Psi \quad (2.1)$$

where \hat{H} is the Hamiltonian operator for system of M nuclei and N electrons in terms of magnetics and electric field there for can be written as (2.2)

$$\hat{H} = -\frac{1}{2} \sum_{i=1}^N \nabla_i^2 - \frac{1}{2} \sum_{A=1}^M \frac{1}{M_A} \nabla_A^2 - \sum_{i=1}^N \sum_{A=1}^M \frac{Z_A}{r_{iA}} + \sum_{i=1}^N \sum_{j>1}^N \frac{1}{r_{ij}} + \sum_{A=1}^M \sum_{B>A}^M \frac{Z_A Z_B}{R_{AB}} \quad (2.2)$$

Equation (2.2) represent to the ground state energy when the first two term describe to kinetic energy of electrons and nuclei, the last tree term remain to the attractive electrostatic interaction between nuclei and electron and repulsive potential among electron-electron and nucleus-nucleus interactions.

Born–Oppenheimer was used to calculate the significant difference between mass of nuclei and electron to describe the Schrödinger equation. The approximation was considered about electron moving faster than, so their kinetic terms be zero. Thus, in equation (2.2) can be reduced to the electronic Hamiltonian in equation (2.3)

$$\hat{H}_{elec} = -\frac{1}{2} \sum_{i=1}^N \nabla_i^2 - \sum_{i=1}^N \sum_{A=1}^N \frac{Z_A}{r_{iA}} + \sum_{i=1}^N \sum_{j>i}^N \frac{1}{r_{ij}} = \hat{T} + \hat{V}_{Ne} + \hat{V}_{ee} \quad (2.3)$$

The total energy is summation of electronic energy and nuclear repulsion term and the constant nuclear repulsion term that depends on electron coordinate.

$$\hat{H}_{elec} \Psi_{elec} = E_{elec} \Psi_{elec} \quad (2.4)$$

and

$$E_{total} = E_{elec} + E_{nuc} \quad (2.5)$$

The second operation V_{Ne} in equation (2.3) is term of the external potential term V_{ext} in DFT method

2.2 HF Approximation

The solution of Schrödinger equation [53] which contain wave function of N electron gives total energy. The wave function which is minimized to lowest energy will be Ψ_0 and the energy will be ground state energy E_0 .

$$E_0 = \min_{\Psi \rightarrow N} E[\Psi] = \min_{\Psi \rightarrow N} \langle \Psi | \hat{T} + \hat{V}_{Ne} + \hat{V}_{ee} | \Psi \rangle \quad (2.6)$$

The ground state wave function enable to determination of ground state energy of system.

The HF was used to approximation of many electronic wave function at ground state. The approximation consists of the N–electron wave function by an anti–symmetrically product of one electron wave function $\chi_i(x_i)$ which product referred to Slater determinant [54], Φ_{SD}

$$\Psi = \frac{1}{\sqrt{N!}} \begin{vmatrix} \chi_1(x_1) & \chi_2(x_2) \dots & \chi_n(x_n) \\ \chi_1(x_2) & \chi_2(x_2) \dots & \chi_n(x_2) \\ \dots & \dots & \dots \\ \chi_1(x_N) & \chi_2(x_N) & \chi_N(x_N) \end{vmatrix} \quad (2.7)$$

where the one electron wave function $\chi_i(x_i)$ is spin orbital which compose of spatial orbital $\Phi_i(r_i)$ and the two spin of wave functions, $\alpha(s)$ and $\beta(s)$. The energy from slater determinant is minimal when the spin orbital are varied under the constraint.

$$E_{HF} = \min_{\Phi_{SD} \rightarrow N} E[\Phi_{SD}] \quad (2.8)$$

The equation (2.9) is a functional of the spin orbitals, $E_{HF} = E[\chi_i]$ that the $E[\chi_i]$ remains to orthonormal, which introduces the Lagrangian multipliers ε_i in the resulting equations.

$$\hat{f}\chi_i = \varepsilon_i \chi_i, i = 1, 2, \dots, N \quad (2.9)$$

This equation (2.10) represent the HF equation, where ε_i are the eigenvalues of the operator \hat{f} . The ε_i is an orbital energy and the Fock operator \hat{f} is an effective one electron operator defined as

$$\hat{f}_i = -\frac{1}{2} \nabla_i^2 - \sum_A \frac{Z_A}{r_{iA}} + V_{HF(i)} \quad (2.10)$$

The first two terms are kinetic energy and V_{HF} is the HF potential. The HF method represents to exchange energy, constitute main obstacle in density functional which the Fock operator depends on the HF potential. A Slater determinant is defined as the sum of the Fock operator in equation (2.10) which uses to determine N interacting electron

$$\hat{H}_{HF}\Phi_{SD} = E_{HF}^0\Phi_{SD} = \sum_i^N \hat{f}_i\Phi_{SD} = \sum_i^N \varepsilon_i\Phi_{SD} \quad (2.11)$$

Equation (2.10) describes a system of N electrons which no interaction of electron–electron. The HF approximation describe under the Coulomb potential and a non–local exchange potential.

2.3 DFT method

The basis for DFT is determination of ground state electronic energy by electron density, ρ [55–58]. The electron density refers to the external potential and Hamilton operator.

The HF model is known as DFT based on the solution of many–electron problem. The HF energy can be written as a sum of the kinetic energy, E_T , the electron–nuclear potential energy, E_V , and coulomb, E_J , and exchange, E_K , as equation (2.13)

$$E^{HF} = E_T + E_V + E_J + E_K \quad (2.12)$$

The first three terms take over directly to density functional models, its energy is replaced by exchange–correlation energy, E_{XC} , the form of which follows from the solution of the idealized electron gas problem

$$E^{DFT} = E_T + E_V + E_J + E_{XC} \quad (2.13)$$

where E_T , all components depend upon the total electron density, $\rho(r)$:

$$\rho(r) = 2 \sum_i^{\text{orbitals}} |\psi_i(r)|^2 \quad (2.14)$$

where ψ_i are orbitals, strictly similar to molecular orbitals in HF theory.

2.3.1 The Kohn–Sham energy and the Kohn–Sham equations

The basic ideas of the Kohn–Sham theory [55] are: (1) to present the molecular energy as a sum of terms involves the “unknown” functional and (2) to use the electron density ρ in the Kohn–Shame equations for calculation of the Kohn–Shame orbitals and energy levels. The final Kohn–Sham orbitals are used to calculate an electron density (ρ).

2.3.1.1 The Kohn–Sham energy

The Kohn–Shame energy [56] was used to separate the electronic energy of molecule into a portion which can be calculate without using DFT. The basic concept in this this approach is the concept of non–interacting system, thus the ground state electron density was defined by ρ_r that the same as real ground state system, $\rho_r = \rho_0$.

The sum of the electron kinetic energy, the nucleus–electron attraction potential energy and the electron–electron repulsion potential energy is the ground state electronic energy of the real molecule, E_0

$$E_0 = \langle T[\rho_0] \rangle + \langle V_{\text{nc}}[\rho_0] \rangle + \langle V_{\text{ec}}[\rho_0] \rangle \quad (2.15)$$

The brackets referred to expectation values of the energy term in quantum–mechanical that is a functional of the ground–state electron density. The middle term was shown the nucleus–electron potential energy in term of sum over all $2n$ electrons, the potential corresponding to attraction of an electron for all the nuclei A:

$$\langle V_{ne} \rangle = \sum_{i=1}^{2n} \sum_{\text{nuclei } A} -\frac{Z_A}{r_{iA}} = \sum_{i=1}^{2n} v(r_i) \quad (2.16)$$

where $\frac{Z_A}{r_{iA}}$ is the potential energy between interaction of electron i and nucleus A at distance r , $v(r_i)$ is the external potential for the attraction of electron i to all the nuclei. The density function ρ in equation (2.14) can be rewritten into V_{Ne} :

$$\int \Psi \sum_{i=1}^{2n} f(r_i) \Psi dt = \int \rho(r) f(r) dr \quad (2.17)$$

where $f(r_i)$ is a function of the coordinates of the $2n$ electrons of a system and Ψ is the total wave function. From equations (2.15) and (2.16) the notion of expectation value, $\langle V_{ne} \rangle = \langle \Psi | \hat{V}_{ne} | \Psi \rangle$, and since $\hat{V} = V_x$ was shown in equation (2.18)

$$\langle V_{ne} \rangle = \int \rho_0(r) v(r) dr \quad (2.18)$$

and the ground state energy was written in equation (2.19)

$$E_0 = \int \rho_0(r) v(r) dr + \langle T[\rho_0] \rangle + \langle V_{ee}[\rho_0] \rangle \quad (2.19)$$

but this equation cannot be used to describe the kinetic and potential energy functionals in terms of $\langle T[\rho_0] \rangle$ and $\langle V_{ee}[\rho_0] \rangle$. The Kohn and Sham idea is the idea of a reference system of non-interacting electrons and lets to know the quantity $\Delta \langle T[\rho_0] \rangle$ as the deviation of the real kinetic energy from that of the reference system.

$$\Delta \langle T[\rho_0] \rangle \equiv \langle T[\rho_0] \rangle - \langle T_r[\rho_0] \rangle \quad (2.20)$$

From the electronic potential energy, $\Delta\langle V_{ee} \rangle$ was defined as the deviation of the real electron–electron repulsion energy from a classical charge cloud coulomb repulsion energy. The classical electrostatic repulsion energy is sum of the repulsion energies for pairs of minimal volume elements $\rho(r_1)dr_1$ and $\rho(r_2)dr_2$ separated by a distance r_{12} , multiplied by one-half.

$$\Delta\langle V_{ee}[\rho_0] \rangle = \langle V_{ee}[\rho_0] \rangle - \frac{1}{2} \iint \frac{\rho_0(r_1)\rho_0(r_2)}{r_{12}} dr_1 dr_2 \quad (2.21)$$

The classical charge-cloud repulsion is inappropriate for electrons because it repulse itself, as any two regions of the cloud interact repulsively. The another way to compensate for this physically incorrect electron self-interaction is a good exchange–correlation functional can be written

$$E_0 = \int \rho_0(r)v(r)dr + \langle T_r[\rho_0] \rangle - \frac{1}{2} \iint \frac{\rho_0(r_1)\rho_0(r_2)}{r_{12}} dr_1 dr_2 + \Delta\langle T[\rho_0] \rangle + \Delta\langle V_{ee}[\rho_0] \rangle \quad (2.22)$$

The major problem with DFT is the summation of the kinetic energy deviation from the reference system and the electron–electron repulsion energy, called the exchange–correlation energy. This exchange–correlation energy, E_{xc} , is a functional of the electron density function;

$$E_{xc}[\rho_0] \equiv \Delta\langle T[\rho_0] \rangle + \Delta\langle V_{ee}[\rho_0] \rangle \quad (2.23)$$

where the $\Delta\langle T \rangle$ term represent to kinetic correlation energy of the electrons and the $\langle \Delta V_{ee} \rangle$ term is the potential correlation and the exchange energy. The ground state energy was became to equation (2.24)

$$E_0 = \int \rho_0 v(r) dr + \langle T[\rho_0] \rangle_{ref} + \frac{1}{2} \iint \frac{\rho_0(r_1)\rho_0(r_2)}{r_{12}} dr_1 dr_2 + E_{xc}[\rho_0] \quad (2.24)$$

equation (2.21) is the Kohn–Sham energy equation.

2.3.1.2 The Kohn–Sham equations

The Kohn–Sham equations [57–58] are derived by differentiating the energy base on the HF equations, where differentiation is with refer to wave function molecular orbitals. The ground state of system was determine by using distribution of the electron density of the reference system, which as same as the ground state of real system, is given by

$$\rho_0 = \rho_r = \sum_{i=1}^{2n} |\psi_i^{\text{KS}}(\mathbf{1})|^2 \quad (2.25)$$

where ψ_i^{KS} are the Kohn–Sham spatial orbital. The Kohn–Shame equation was determine by substituting of the orbitals into the energy and varying E_0 with respect to the ψ_i^{KS} , this procedure is the same of the HF equations,

$$\left[-\frac{1}{2}\nabla_i^2 - \sum_{\text{nuclei } A} \frac{Z_A}{r_{iA}} + \int \frac{\rho(r_2)}{r_{12}} dr_2 + V_{\text{xc}}(\mathbf{1}) \right] \psi_i^{\text{KS}}(\mathbf{1}) = \varepsilon_i^{\text{KS}} \psi_i^{\text{KS}}(\mathbf{1}) \quad (2.26)$$

where $\varepsilon_i^{\text{KS}}$ are the Kohn–Sham energy levels and $v_{\text{xc}}(\mathbf{1})$ is the exchange correlation potential which is defined as the functional derivative of $E_{\text{xc}}[\rho_0(r)]$ with respect to $\rho(r)$;

$$v_{\text{xc}}(r) = \frac{\delta E_{\text{xc}}[\rho(r)]}{\delta \rho(r)} \quad (2.27)$$

The Kohn–Sham theory $\rho(r)$ is expressed in terms of Kohn–Sham orbitals (Eq. 2.25), are discussed by Parr and Yang [59] and outlined by Levine [49].

$$\hat{h}^{\text{KS}}(\mathbf{1})\psi_i^{\text{KS}}(\mathbf{1}) = \varepsilon_i^{\text{KS}}\psi_i^{\text{KS}}(\mathbf{1}) \quad (2.28)$$

The difference between DFT methods is the choice of the functional from of the exchange–correlation energy. Functional forms are often designed to have a certain limiting behavior, and correct parameters to known perfect data. Which functional is the better will have to be settled by comparing the performance with experiments or high–level wave mechanics calculations.

The Kohn–Sham equations give the correct energy if we knew the exact exchange correlation energy functional.

2.4 Gaussian basis sets

A basis set is a set of mathematical functions (basis functions). The approximation of molecular orbitals as linear combinations of basis functions is usually called the linear combination of atomic orbitals or LCAO. The basis functions was used to describe the electron distribution around atom and combining atomic basis functions.

2.4.1 Linear combination of atomic orbitals

The LCAO approximation [54] requires the use of a basis set made up of a finite number of well–defined functions centered on each atom. This functions was not cost effective, and early numerical calculations were carried out using Slater–type orbitals (STOs), defined by

$$\phi(r, \theta, \phi) = \frac{(2\zeta / a_0)^{n+1/2}}{[(2n)!]^{1/2}} r^{n-1} e^{-\zeta r/a_0} Y_l^m(\theta, \phi) \quad (2.29)$$

where the notation of n , m , and l was shown the usual quantum numbers and ζ are the effective nuclear charge. Further work revealed that the cost of calculations can be further reduced if the AOs are expanded in terms of Gaussian functions, which have the form in equation (2.30)

$$g_{ijk}(r) = Nx^i y^j z^k e^{-\alpha r^2} \quad (2.30)$$

where x , y , and z are the position coordinates from the nucleus of an atom; i , j , and k are nonnegative integers, and α is an orbital exponent.

The solution of the STOs by a linear combination was used to approximate Gaussian functions that function has a different α values, more than by a single Gaussian function. These linear combinations was called contracted functions that became to the elements of basis set.

2.4.2 Minimal basis sets

The minimal basis sets [53–54] have been studied under STO–3G basis set. These basis functions is extended in terms of three Gaussian functions The values of the Gaussian exponents and the linear coefficient have been determined by least squares as best fits to Slater–type (exponential) functions.

$$\begin{aligned} \phi(2s) &= d_{1s} e^{-\alpha_{1s} r} + d_{2s} e^{-\alpha_{2s} r} + d_{3s} e^{-\alpha_{3s} r} \\ \phi(2p_x) &= d_{1p_x} e^{-\alpha_{1p} r} + d_{2p_x} e^{-\alpha_{2p} r} + d_{3p_x} e^{-\alpha_{3p} r} \\ \phi(2p_y) &= d_{1p_y} e^{-\alpha_{1p} r} + d_{2p_y} e^{-\alpha_{2p} r} + d_{3p_y} e^{-\alpha_{3p} r} \\ \phi(2p_z) &= d_{1p_z} e^{-\alpha_{1p} r} + d_{2p_z} e^{-\alpha_{2p} r} + d_{3p_z} e^{-\alpha_{3p} r} \end{aligned}$$

2.4.3 Split–valence basis sets

The Split–valence basis sets [55–57] presents core atomic orbitals by one set of functions and valence atomic orbitals. The basic of a split–valence basis sets are 3–21G and 6–31G. Each core atomic orbital in the 3–21G basis set is extended in terms of three Gaussians, on the other hand a basis functions represent to inner and outer components of valence atomic orbitals which expanded in term of two and one Gaussians. The 6–31G basis sets are the same constructed which core orbitals was presented in terms of six Gaussians and valence orbitals split into three and one Gaussians components. The expansion coefficients and Gaussians exponents for

3–21G and 6–31G basis sets have been investigated by HF energy minimization on atomic ground states.

2.4.4 Polarized basis sets

The polarization functions [55–57] can be included in terms of hybrid orbitals, (i.e., pd and sp hybrids) and in terms of a Taylor series expansion of a function. The simplest polarization basis set is 6–31G*, raised from 6–31G by adding a set of d -type polarization functions and set of six second-order Gaussians is added in the case of 6–31G*. The Gaussian exponential for polarization functions have been used to give the lowest energies for representative molecules. Polarization of the s orbitals on hydrogen atoms is necessary for description of the bonding in many systems.

2.4.5 Basis sets incorporating diffuse functions

The diffusion function [55–57] can be used to expand the highest energy electron systems. The basis sets may use to be supplemented by diffuse functions, such as diffuse s - and p -type functions. The 6–31+G (d) basis set was added to heavy atoms and the double plus description, 6–31++G(d), added to the hydrogen atoms. The diffuse functions can also be added along with polarization functions, for example, to the 6-31+G*, 6-31++G*, 6-31+G** and 6-31++G** basis sets.

2.5 The potential energy surface

The PES [55, 56] is main concept in computational chemistry because this concept can be used to visualization and explanation of the relationship between potential energy and molecular geometry by using a plot of the energy of nuclei and electrons with the geometric coordinates of the nuclei.

The Born–Oppenheimer is a very good approximation the nuclei in a molecule. The approximation base on the Schrödinger equation, a molecule may be separated into an electronic and a nuclear equation. The solution of electronic Schrödinger equation was used to calculate energy of molecule and then add the electronic energy to the internuclear repulsion to get the total internal energy. The

PES concept are in valid when nuclear coordinates was fixed that the concepts of molecular geometry or shape.

The PES calculation may be called a Born–Oppenheimer surface that can be represent to the geometries and the corresponding energies of a collection of atomic nuclei. The PES scan was shown the global and local minimum of structure from geometry optimization.

CHAPTER III

DETAILS OF THE CALCULATIONS

3.1 Computational method

Geometry optimizations of the pristine and defective graphene and GOs were performed using the DFT/B3LYP method [60–62]. Configurations of di-hydroxide in GOs were obtained by PES method using semi-empirical AM1 method [63] and their structures were reoptimized at the B3LYP/6–31G(d,p) level of theory. Optimizations for system of oxygen atom, their doublet state were applied. All calculations were investigated under the GAUSSIAN 03 program [64].

Adsorption energies (ΔE_{ads}) of oxygen and hydrogen peroxide molecules on basal plane of GO are defined by equations (3.1) and (3.2), respectively.

$$\Delta E_{\text{ads}} = E_{(\text{O})_2\text{G}} - (E_{\text{G}} + E_{\text{O}_2}) \quad (3.1)$$

$$\Delta E_{\text{ads}} = E_{(\text{OH})_2\text{G}} - (E_{\text{G}} + E_{\text{H}_2\text{O}_2}) \quad (3.2)$$

where $E_{(\text{O})_2\text{G}}$, E_{G} and E_{O_2} are total energies of epoxy GO, strained graphene and free oxygen molecule, respectively. $E_{(\text{OH})_2\text{G}}$ and $E_{\text{H}_2\text{O}_2}$ are total energies of di-hydroxyl GO and free hydrogen peroxide molecule, respectively.

Reaction energies (ΔE_{react}) of graphene oxidation to produce carbonyl and carboxyl GOs are defined by equations (3.3) and (3.4), respectively.

Carbonylation:

$$\Delta E_{\text{react}} = (E_{(\text{OC})_2\text{C}_{78}\text{H}_{20}} + E_{\text{H}_2}) - (E_{\text{C}_{80}\text{H}_{22}} + E_{\text{O}_2}) \quad (3.3)$$

Carboxylation:

$$\Delta E_{\text{react}} = E_{\text{HOOC}_79\text{H}_{21}} - (E_{\text{C}_{80}\text{H}_{22}} + E_{\text{O}_2}) \quad (3.4)$$

where $E_{(\text{OC})_2\text{C}_{78}\text{H}_{20}}$, $E_{\text{HOOC}_79\text{H}_{21}}$ and $E_{\text{C}_{80}\text{H}_{22}}$ are total energies of carbonyl GO, carboxyl GO and graphene, respectively. E_{H_2} is total energy of hydrogen molecule.

Formation energies (ΔE_{form}) for n oxygen molecules and m hydrogen peroxide molecules on basal plane of GO as one (top side, GO') and both (top and bottom sides, GO'') sides are defined by equations (3.5) and (3.6), respectively. The strain energies of graphenes in form of GO' ($\Delta E_{\text{strain}}(\text{GO}')$) and GO'' ($\Delta E_{\text{strain}}(\text{GO}'')$) are computed by equations (3.7) and (3.8), respectively.

$$\Delta E_{\text{form}}(\text{GO}') = E_{\text{GO}'} - (E_{\text{G}} + nE_{\text{O}_2} + mE_{\text{H}_2\text{O}_2}) \quad (3.5)$$

$$\Delta E_{\text{form}}(\text{GO}'') = E_{\text{GO}''} - (E_{\text{G}} + nE_{\text{O}_2} + mE_{\text{H}_2\text{O}_2}) \quad (3.6)$$

$$\Delta E_{\text{strain}}(\text{GO}') = E_{\text{G}_{\text{GO}'}} - E_{\text{G}_{\text{free}}} \quad (3.7)$$

$$\Delta E_{\text{strain}}(\text{GO}'') = E_{\text{G}_{\text{GO}''}} - E_{\text{G}_{\text{free}}} \quad (3.8)$$

where $E_{\text{G}_{\text{GO}'}}$ and $E_{\text{G}_{\text{GO}''}}$ are total energies of graphenes in forms of GO' and GO'', respectively. $E_{\text{G}_{\text{free}}}$ is total energy of isolated graphene sheet.

3.2 Cluster models

Two sizes of graphene clusters, $\text{C}_{80}\text{H}_{22}$ and $\text{C}_{96}\text{H}_{24}$ were employed for three cluster models. Larger size of graphene cluster, $\text{C}_{96}\text{H}_{24}$ was employed as Model 1 (noted GM1) of which interaction area is the perfect C_{54} subcluster (coronene-like cluster), in order to get more accurate results of interaction in vicinity of hexagonal center instead of bond center of Model 2. The $\text{C}_{80}\text{H}_{22}$ cluster was used for Model 2 and Model 3 of which interaction areas are the perfect C_{42} subcluster and the Stone–Wales defect (SW) [65] C_{42} subcluster, respectively. The centers of subcluster for

perfect and SW-defective graphenes are a pyrene-like (C16) and a 5-7-7-5 (C16) clusters, respectively. The Model 2 and Model 3 are also noted as GM2 and GM3, respectively, as shown in Figure 3.1 Model 4 and Model 5 are defined as C₈₀H₂₂ cluster of which flexible areas are pyrene-like cluster located at C-C bond of armchair edge and tetracene-like cluster located at C-C bond of zigzag edge, respectively.

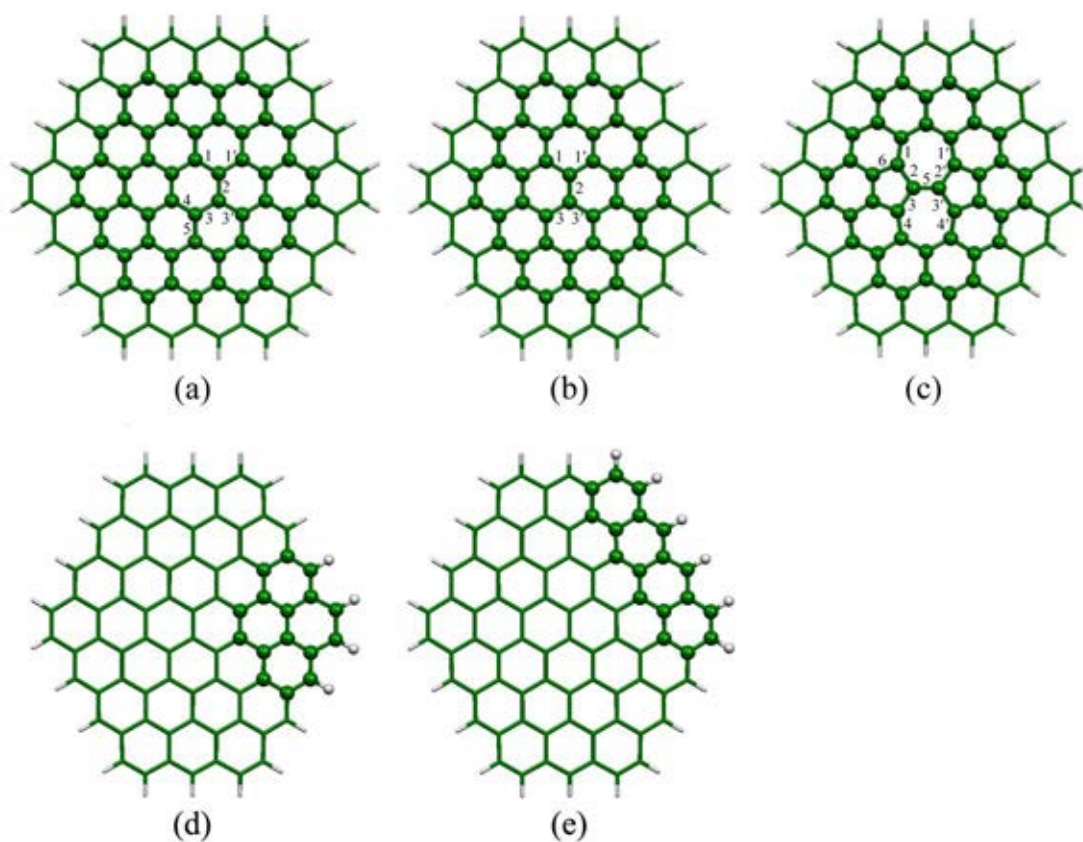


Figure 3.1 Cluster models for (a) pristine graphene, Model 1 or GM1 (C₅₄ in C₉₆H₂₄ cluster), (b) pristine graphene, Model 2 or GM2 (C₄₂ in C₈₀H₂₂ cluster), (c) SW-defective graphene, Model 3 or GM3 (C₄₂ in C₈₀H₂₂ cluster), (d) Model 4 and (e) Model 5. Ball atoms are defined as flexible atoms treated in optimization; the rest atoms are frozen. C-C bonds labeling is used in di-epoxide GOs notation.

3.3 Definition of oxidation for producing GO

Oxidations of graphene to produce epoxy and hydroxyl GOs are defined adsorption of oxygen and hydrogen peroxide molecules on basal plane, respectively. For oxidations to produce carbonyl and carboxyl GOs are defined as reaction of oxygen and hydrogen molecules at graphene edge. The oxidations to produced GOs are therefore defined as follows.

- (i) Two epoxy groups formed on graphene due to an oxygen molecule adsorption during oxidation process are assumed.
- (ii) Two hydroxyl groups formed on graphene due to a hydrogen peroxide molecule adsorption during oxidation process are assumed.
- (iii) Overall reactions of carbonylation and carboxylation on graphene are defined by equations (3.9) and (3.10), respectively.



where $\text{C}_{80}\text{H}_{22}$ is graphene sheet which is defined as a cluster Model 4.

3.4 PES scans for di-hydroxyl GO

PESs for interactions between of two hydroxyl groups in GO were scanned using semi-empirical AM1 method. The PESs for di-hydroxyl GOs are shown in Figure A-2, in appendix for perfect graphene (Model 2) and Figure A-3 for SW-defective graphene (Model 3).

3.5 Notations for GOs

Notation for di-epoxide GO is defined as $\underline{O}^{\text{bond\#1}}, O^{\text{bond\#2}}/\text{GM}(\#)$, where bond#1 and bond#2 are bond numbers as defined in Figure 3.1 and GM(#) is graphene model #. GM1, GM2 and GM3 are therefore graphene Model 1, Model 2 and Model 3, as shown in Figure 3.1 (a), (b) and (c), respectively. Underline O atom in $\underline{O}^{\text{bond\#1}}, O^{\text{bond\#2}}/\text{GM}(\#)$ notation means that this O atom is located on opposite side of graphene sheet. Notation for di-hydroxyl GO is defined as $(\text{OH})_2(\#)/\text{GM}(\#)$ where # in $(\text{OH})_2(\#)$ is running number for GO configuration. For graphene reacts in oxidation, the $\text{C}_{42}\text{H}_{22}$ cluster as Model 2 is employed as graphene sheet. The carbonyl GO and carboxyl GO are therefore represented with $(\text{OC})_2-\text{C}_{78}\text{H}_{20}$ and $\text{HOOC}-\text{C}_{79}\text{H}_{21}$, respectively.

CHAPTER IV

RESULTS AND DISCUSSION

In the present study, all possible functionalized structures of graphene with oxygen-containing groups were presented. The cluster models such as $C_{80}H_{22}$ (Model 2 with C_{42} subcluster and Model 3 with Stone–Wales C_{42} subcluster) and $C_{96}H_{24}$ (Model 1 with C_{54} subcluster), these cluster models were functionalized with di-epoxide from oxygen and di-hydroxide from hydrogen peroxide on the basal plane. In the other hand, carboxyl and carbonyl groups were presented at edge of graphene their structure were presented in model 4 and model 5. The adsorption energy and electronic properties of GO have been investigated. The results and discussion were shown at below.

4.1 Conformations for epoxy GO

All possible configurations of di-epoxide on pristine graphene sheets are shown in Figure 4.1. Relative energies of configurations of di-epoxide GOs compared with the lowest energies for each computational models are shown in Table 4.1 and their selected geometrical parameters for configurations of di-epoxide GOs are shown in Table A-1. The Table 4.1 shows that $O^1\underline{Q}^3/GM1$ and $O^6\underline{Q}^3/GM3$ are the most stable configurations of di-epoxide GOs using Model 1 and Model 3, respectively. The two configurations of which relative energies are slightly different which is less than 1 kcal/mol are $O^1\underline{Q}^3/GM1$ and $O^{1*}\underline{Q}^2/GM1$ for pristine graphene system and $O^6\underline{Q}^3/GM3$ and $O^2\underline{Q}^{2'}/GM3$ for SW-defective graphene system. As energy gap depends on chemical reactivity, it may be conclude that $O^1\underline{Q}^3/GM1$ ($E_{gap}=1.10$ eV) is more reactive than $O^{1*}\underline{Q}^2/GM1$ ($E_{gap}=1.69$ eV) and $O^6\underline{Q}^3/GM3$ ($E_{gap}=1.25$ eV) is more reactive than $O^2\underline{Q}^{2'}/GM3$ ($E_{gap}=1.88$ eV).

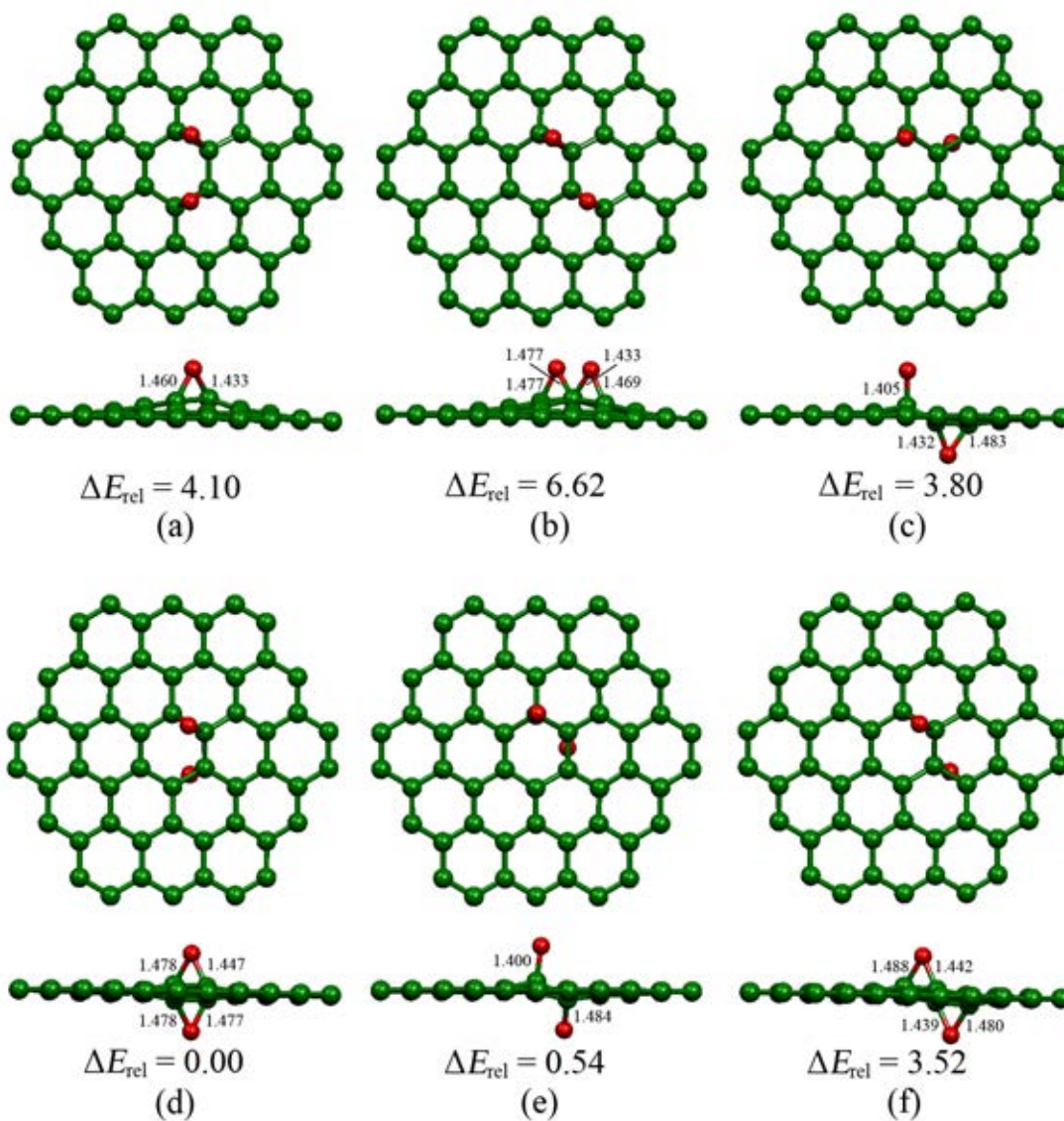


Figure 4.1 Configurations of di-epoxide in vicinity of pristine graphene sheets center, noted as (a) $O^1O^3/GM1$, (b) $O^1Q^3'/GM1$, (c) $O^1*Q^1'/GM1$, (d) $O^1Q^3/GM1$, (e) $O^1*Q^2/GM1$ and (f) $O^1Q^3'/GM1$. Their relative energies and bond lengths are in kcal/mol and Å, respectively.

Table 4.1 Relative energies of configurations of di-epoxy GOs compared with lowest energies for each cluster models, their frontier orbital energies and energy gaps.

Species	$\Delta E_{\text{rel}}^{\text{a}}$	$E_{\text{LUMO}}^{\text{b}}$	$E_{\text{HOMO}}^{\text{b}}$	$E_{\text{gap}}^{\text{b}}$
<i>Model 1:</i>				
O ¹ O ³ /GM1	4.10	-2.64	-3.66	1.02
O ¹ <u>O</u> ³ /GM1	6.62	-2.61	-3.79	1.18
O ¹ * <u>O</u> ¹ /GM1	3.80	-2.74	-4.31	1.57
O ¹ <u>O</u> ³ /GM1	0.00	-2.62	-3.72	1.10
O ¹ * <u>O</u> ² /GM1	0.54	-2.64	-4.33	1.69
O ¹ <u>O</u> ³ /GM1	3.52	-2.69	-3.77	1.08
<i>Model 3:</i>				
O ² O ² /GM3	13.99	-2.68	-4.54	1.86
O ² O ³ /GM3	18.67	-2.86	-3.84	0.98
O ¹ O ³ /GM3	6.76	-2.67	-3.74	1.07
O ¹ O ⁵ /GM3	10.65	-2.62	-4.10	1.48
O ⁶ O ² /GM3	7.57	-2.53	-3.75	1.22
O ² O ³ /GM3	22.03	-3.00	-4.26	1.27
O ² <u>O</u> ² /GM3	0.39	-2.69	-4.56	1.88
O ⁶ <u>O</u> ⁵ /GM3	8.03	-2.85	-3.74	0.89
O ¹ <u>O</u> ³ /GM3	5.64	-2.68	-3.79	1.11
O ¹ <u>O</u> ⁵ /GM3	11.16	-2.62	-4.17	1.55
O ⁶ <u>O</u> ³ /GM3	0.00	-2.49	-3.74	1.25
O ⁶ <u>O</u> ⁵ /GM3	18.74	-3.01	-4.37	1.36

^a In kcal/mol.

^b In eV.

The most stable configuration of GM1 is O¹O³/GM1, its total energy is -3823.65715494 au. and GM3 shows that the most stable configuration is O⁶O³/GM3, its total energy is -3212.49499330 au.

All possible configurations of di-epoxide in vicinity of SW-defective in graphene sheets are shown in Figure 4.2. The adsorption energies of oxygen molecule on the graphene basal plane to afford epoxy GOs and strain energies of their graphene sheets are shown in Table 4.2. The adsorption energies of oxygen on pristine and SW-defective graphenes as epoxy GOs are within the range of -22.43 to -1.52 and -42.39 to -24.82 kcal/mol, respectively. The strain energies of s pristine and SW-defective graphenes are within the range of 33.79 to 44.74 and 30.57 to 48.50 kcal/mol, respectively. The most stable configuration for di-epoxy pristine and

di- epoxy SW-defective GOs are $O^1O^3/GM1$ and $O^6O^3/GM3$, respectively of which corresponding adsorption energies are -9.36 and -42.39 kcal/mol, respectively.

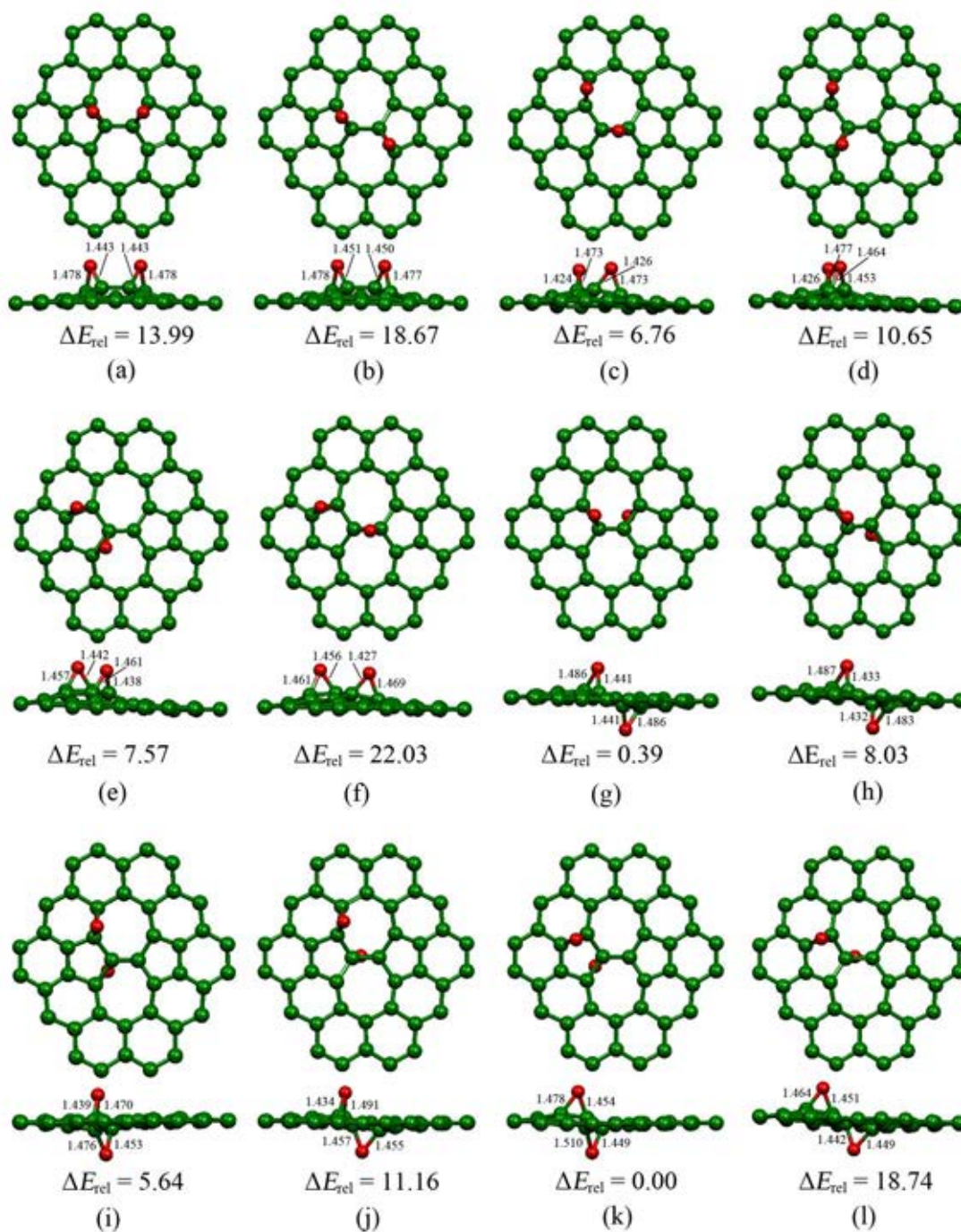


Figure 4.2 Configurations of di-epoxides in vicinity of SW-defective graphene sheets noted (a) $O^2O^2/GM3$, (b) $O^2O^3/GM3$, (c) $O^1O^3/GM3$, (d) $O^1O^5/GM3$, (e) $O^6O^2/GM3$, (f) $O^2O^3/GM3$, (g) $O^2O^2/GM3$, (h) $O^6O^5/GM3$, (i) $O^1O^3/GM3$, (j)

$O^1\underline{O}^5/GM3$, (k) $O^6\underline{O}^3/GM3$ and (l) $O^6\underline{O}^5/GM3$. Their relative energies and bond lengths are in kcal/mol and Å, respectively.

Table 4.2 Adsorption energies of oxygen molecule on the graphene basal plane to afford epoxy GOs and strain energies of their graphene sheets.

Adsorption	ΔE_{ads}^a	$\Delta E_{\text{strain}}^a$
Model 1:		
GM1(1) + O ₂ → O ¹ O ³ /GM1	-12.02	41.65
GM1(2) + O ₂ → O ¹ <u>O^{3'}/GM1</u>	-4.52	36.66
GM1(3) + O ₂ → O ^{1*} <u>O^{1'}/GM1</u>	-18.54	47.87
GM1(4) + O ₂ → O ¹ <u>O³/GM1</u>	-9.36	34.88
GM1(5) + O ₂ → O ^{1*} <u>O²/GM1</u>	-22.43	48.50
GM1(6) + O ₂ → O ¹ <u>O^{3'}/GM1</u>	-1.52	30.57
Model 3:		
GM3(1) + O ₂ → O ² O ^{2'} /GM3	-34.97	44.74
GM3(2) + O ₂ → O ² O ^{3'} /GM3	-24.90	39.35
GM3(3) + O ₂ → O ¹ O ³ /GM3	-33.84	36.37
GM3(4) + O ₂ → O ¹ O ⁵ /GM3	-33.11	39.54
GM3(5) + O ₂ → O ⁶ O ² /GM3	-32.40	35.75
GM3(6) + O ₂ → O ² O ^{3'} /GM3	-25.79	43.59
GM3(7) + O ₂ → O ² <u>O^{2'}/GM3</u>	-39.07	35.24
GM3(8) + O ₂ → O ⁶ <u>O⁵/GM3</u>	-31.02	34.83
GM3(9) + O ₂ → O ¹ <u>O³/GM3</u>	-32.37	37.79
GM3(10) + O ₂ → O ¹ <u>O⁵/GM3</u>	-30.83	37.77
GM3(11) + O ₂ → O ⁶ <u>O³/GM3</u>	-42.39	38.17
GM3(12) + O ₂ → O ⁶ <u>O⁵/GM3</u>	-24.82	39.34

^a In kcal/mol.

4.2 Conformations for hydroxyl GO

All possible configurations of di-hydroxide on pristine graphene sheets are shown in Figure 4.3. Relative energies of configurations of di-hydroxyl GOs compared with lowest energies for each cluster models are shown in Table 4.3 and their selected geometrical parameters for configurations of di-hydroxyl GOs are shown in Table A-2.

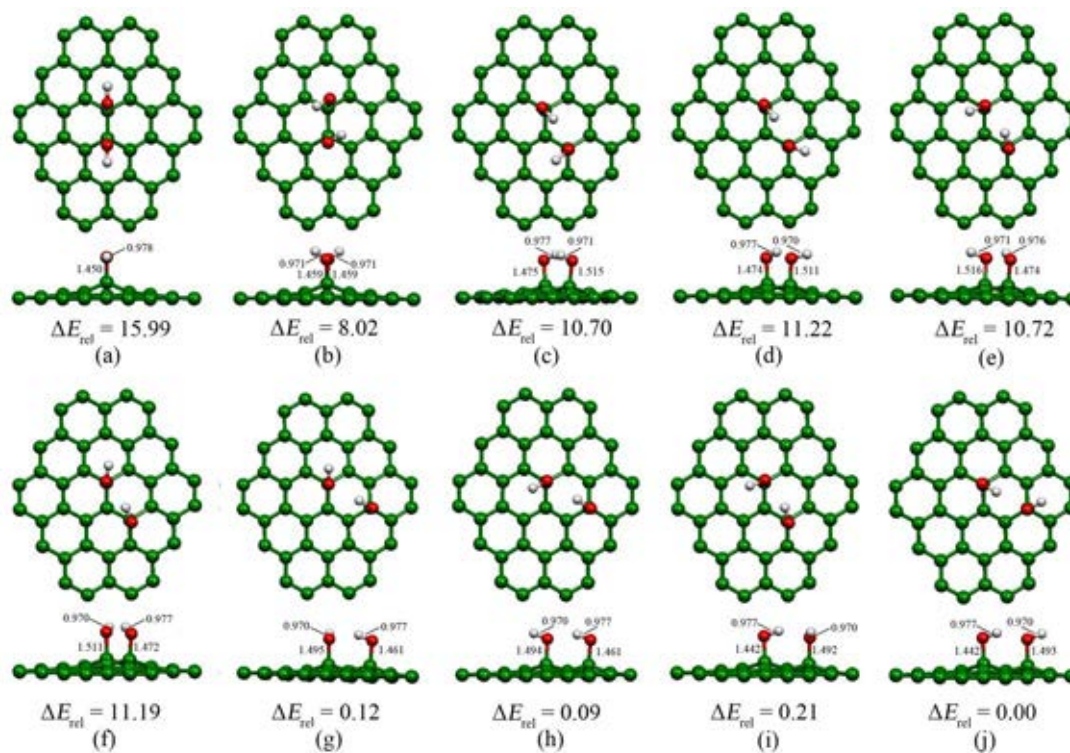


Figure 4.3 Configurations of di-hydroxide on pristine graphene sheets, noted as (a) $(OH)_2(1)/GM2$, (b) $(OH)_2(2)/GM2$, (c) $(OH)_2(3)/GM2$, (d) $(OH)_2(4)/GM2$, (e) $(OH)_2(5)/GM2$, (f) $(OH)_2(6)/GM2$, (g) $(OH)_2(7)/GM2$, (h) $(OH)_2(8)/GM2$, (i) $(OH)_2(9)/GM2$ and (j) $(OH)_2(10)/GM2$. Their relative energies and bond lengths are in kcal/mol and Å, respectively.

Table 4.3 Relative energies of configurations of di-hydroxyl GOs compared with lowest energies for each cluster models, their frontier orbital energies and energy gaps.

Species	$\Delta E_{\text{rel}}^{\text{a}}$	$E_{\text{LUMO}}^{\text{b}}$	$E_{\text{HOMO}}^{\text{b}}$	$E_{\text{gap}}^{\text{b}}$	
Model 2:					
Scan #1:	(OH) ₂ (1)/GM2	15.99	-2.71	-3.55	0.84
	(OH) ₂ (2)/GM2	8.02	-2.71	-3.53	0.82
Scan #2:	(OH) ₂ (3)/GM2	10.70	-2.65	-4.40	1.75
	(OH) ₂ (4)/GM2	11.22	-2.65	-4.41	1.76
	(OH) ₂ (5)/GM2	10.72	-2.67	-4.40	1.73
	(OH) ₂ (6)/GM2	11.19	-2.68	-4.40	1.72
Scan #3:	(OH) ₂ (7)/GM2	0.12	-2.49	-3.72	1.23
	(OH) ₂ (8)/GM2	0.09	-2.49	-3.72	1.24
	(OH) ₂ (9)/GM2	0.21	-2.50	-3.69	1.18
	(OH) ₂ (10)/GM2	0.00	-2.50	-3.70	1.20
Model 3:					
Scan #4:	(OH) ₂ (1)/GM3	15.57	-3.07	-4.47	1.40
	(OH) ₂ (2)/GM3	16.54	-2.74	-3.51	0.77
Scan #5:	(OH) ₂ (3)/GM3	6.73	-2.71	-4.16	1.45
	(OH) ₂ (4)/GM3	6.30	-2.77	-4.11	1.34
Scan #6:	(OH) ₂ (5)/GM3	0.27	-2.33	-3.71	1.37
	(OH) ₂ (6)/GM3	0.00	-2.31	-3.68	1.37
Scan #7:	(OH) ₂ (7)/GM3	23.19	-2.63	-3.49	0.86
Scan #8:	(OH) ₂ (8)/GM3	16.54	-2.57	-3.81	1.24
Scan #9:	(OH) ₂ (9)/GM3	19.92	-2.63	-4.26	1.63
	(OH) ₂ (10)/GM3	19.64	-2.63	-4.27	1.64
	(OH) ₂ (11)/GM3	19.31	-2.57	-4.29	1.72
	(OH) ₂ (12)/GM3	20.13	-2.58	-4.29	1.71
Scan #10:	(OH) ₂ (13)/GM3	17.57	-2.62	-4.25	1.64
	(OH) ₂ (14)/GM3	17.01	-2.66	-4.21	1.55
	(OH) ₂ (15)/GM3	17.42	-2.64	-4.25	1.62
	(OH) ₂ (16)/GM3	16.75	-2.63	-4.24	1.61
	(OH) ₂ (17)/GM3	17.01	-2.66	-4.21	1.55
Scan #11:	(OH) ₂ (18)/GM3	19.12	-2.72	-4.06	1.34
	(OH) ₂ (19)/GM3	20.08	-2.75	-4.06	1.31
Scan #12:	(OH) ₂ (20)/GM3	4.34	-2.35	-3.71	1.36
	(OH) ₂ (21)/GM3	3.73	-2.33	-3.73	1.40
	(OH) ₂ (22)/GM3	3.73	-2.33	-3.73	1.40
	(OH) ₂ (23)/GM3	4.34	-2.35	-3.71	1.36
Scan #13:	(OH) ₂ (24)/GM3	16.58	-2.57	-3.81	1.24
	(OH) ₂ (25)/GM3	16.62	-2.49	-3.80	1.31
Scan #14:	(OH) ₂ (26)/GM3	14.36	-2.79	-4.10	1.31
	(OH) ₂ (27)/GM3	14.70	-2.81	-4.11	1.30
	(OH) ₂ (28)/GM3	14.00	-2.77	-4.15	1.37
Scan #15:	(OH) ₂ (29)/GM3	23.71	-2.71	-3.82	1.10
	(OH) ₂ (30)/GM3	23.14	-2.70	-3.81	1.11
	(OH) ₂ (31)/GM3	23.71	-2.71	-3.82	1.10
Scan #16:	(OH) ₂ (32)/GM3	25.88	-2.50	-4.09	1.60
	(OH) ₂ (33)/GM3	25.97	-2.49	-4.09	1.60
	(OH) ₂ (34)/GM3	25.82	-2.48	-4.10	1.62

^a In kcal/mol.

^b In eV.

The most stable configuration of GM2 is $(\text{OH})_2(10)/\text{GM2}$, its total energy is -3213.88111251 au. and the most stable configuration of GM3 is $(\text{OH})_2(6)/\text{GM3}$, its total energy is -3213.77303232 au.

Adsorption energies of hydrogen peroxide molecule onto the graphene basal plane to afford hydroxyl GOs and strain energies of their graphene sheets are shown in Table 4.4. The adsorption energies of hydrogen peroxide on pristine and SW-defective graphenes as hydroxyl GOs are within the range of -47.55 to -30.742 and -78.80 to -46.58 kcal/mol, respectively.

The most stable configuration for di-hydroxyl pristine and di-hydroxyl SW-defective GOs are $(\text{OH})_2(10)/\text{GM2}$ and $(\text{OH})_2(6)/\text{GM3}$, respectively of which corresponding adsorption energies are -46.47 and -78.80 kcal/mol, respectively. All possible configurations of di-hydroxide in vicinity of SW-defective in graphene sheets are shown in Figure 4.4 and 4.5

Table 4.4 Adsorption energies of hydrogen peroxide molecule onto the graphene basal plane to afford hydroxyl GOs and strain energies of their graphene sheets.

Adsorption	ΔE_{ads}^a	$\Delta E_{\text{strain}}^a$
Model 2:		
GM2(1) + H ₂ O ₂ → (OH) ₂ (1)/GM2	-39.11	69.39
GM2(2) + H ₂ O ₂ → (OH) ₂ (2)/GM2	-47.55	69.85
GM2(3) + H ₂ O ₂ → (OH) ₂ (3)/GM2	-33.05	58.03
GM2(4) + H ₂ O ₂ → (OH) ₂ (4)/GM2	-31.78	57.28
GM2(5) + H ₂ O ₂ → (OH) ₂ (5)/GM2	-30.74	55.75
GM2(6) + H ₂ O ₂ → (OH) ₂ (6)/GM2	-32.44	57.91
GM2(7) + H ₂ O ₂ → (OH) ₂ (7)/GM2	-47.08	61.48
GM2(8) + H ₂ O ₂ → (OH) ₂ (8)/GM2	-47.05	61.41
GM2(9) + H ₂ O ₂ → (OH) ₂ (9)/GM2	-46.37	60.86
GM2(10) + H ₂ O ₂ → (OH) ₂ (10)/GM2	-46.47	60.75
Model 3:		
GM3(1) + H ₂ O ₂ → (OH) ₂ (1)/GM3	-66.42	70.28
GM3(2) + H ₂ O ₂ → (OH) ₂ (2)/GM3	-72.64	77.47
GM3(3) + H ₂ O ₂ → (OH) ₂ (3)/GM3	-71.55	66.57
GM3(4) + H ₂ O ₂ → (OH) ₂ (4)/GM3	-72.71	67.31
GM3(5) + H ₂ O ₂ → (OH) ₂ (5)/GM3	-77.14	65.69
GM3(6) + H ₂ O ₂ → (OH) ₂ (6)/GM3	-78.80	67.09
GM3(7) + H ₂ O ₂ → (OH) ₂ (7)/GM3	-58.50	69.98
GM3(8) + H ₂ O ₂ → (OH) ₂ (8)/GM3	-59.12	63.95
GM3(9) + H ₂ O ₂ → (OH) ₂ (9)/GM3	-53.88	62.09
GM3(10) + H ₂ O ₂ → (OH) ₂ (10)/GM3	-52.88	60.81
GM3(11) + H ₂ O ₂ → (OH) ₂ (11)/GM3	-54.68	62.28
GM3(12) + H ₂ O ₂ → (OH) ₂ (12)/GM3	-54.91	63.33
GM3(13) + H ₂ O ₂ → (OH) ₂ (13)/GM3	-49.05	54.91
GM3(14) + H ₂ O ₂ → (OH) ₂ (14)/GM3	-58.34	63.65
GM3(15) + H ₂ O ₂ → (OH) ₂ (15)/GM3	-50.19	55.91
GM3(16) + H ₂ O ₂ → (OH) ₂ (16)/GM3	-55.75	60.79
GM3(17) + H ₂ O ₂ → (OH) ₂ (17)/GM3	-59.03	64.33
GM3(18) + H ₂ O ₂ → (OH) ₂ (18)/GM3	-47.50	54.91
GM3(19) + H ₂ O ₂ → (OH) ₂ (19)/GM3	-47.54	55.91
GM3(20) + H ₂ O ₂ → (OH) ₂ (20)/GM3	-65.22	57.86
GM3(21) + H ₂ O ₂ → (OH) ₂ (21)/GM3	-66.15	58.17
GM3(22) + H ₂ O ₂ → (OH) ₂ (22)/GM3	-68.50	60.52
GM3(23) + H ₂ O ₂ → (OH) ₂ (23)/GM3	-67.42	60.06
GM3(24) + H ₂ O ₂ → (OH) ₂ (24)/GM3	-59.59	64.46
GM3(25) + H ₂ O ₂ → (OH) ₂ (25)/GM3	-54.95	59.86
GM3(26) + H ₂ O ₂ → (OH) ₂ (26)/GM3	-56.87	59.52
GM3(27) + H ₂ O ₂ → (OH) ₂ (27)/GM3	-57.68	60.67
GM3(28) + H ₂ O ₂ → (OH) ₂ (28)/GM3	-57.65	59.94
GM3(29) + H ₂ O ₂ → (OH) ₂ (29)/GM3	-48.64	60.65
GM3(30) + H ₂ O ₂ → (OH) ₂ (30)/GM3	-47.35	58.78
GM3(31) + H ₂ O ₂ → (OH) ₂ (31)/GM3	-48.86	60.86
GM3(32) + H ₂ O ₂ → (OH) ₂ (32)/GM3	-48.06	62.23
GM3(33) + H ₂ O ₂ → (OH) ₂ (33)/GM3	-46.58	60.84
GM3(34) + H ₂ O ₂ → (OH) ₂ (34)/GM3	-48.56	62.68

^a In kcal/mol.

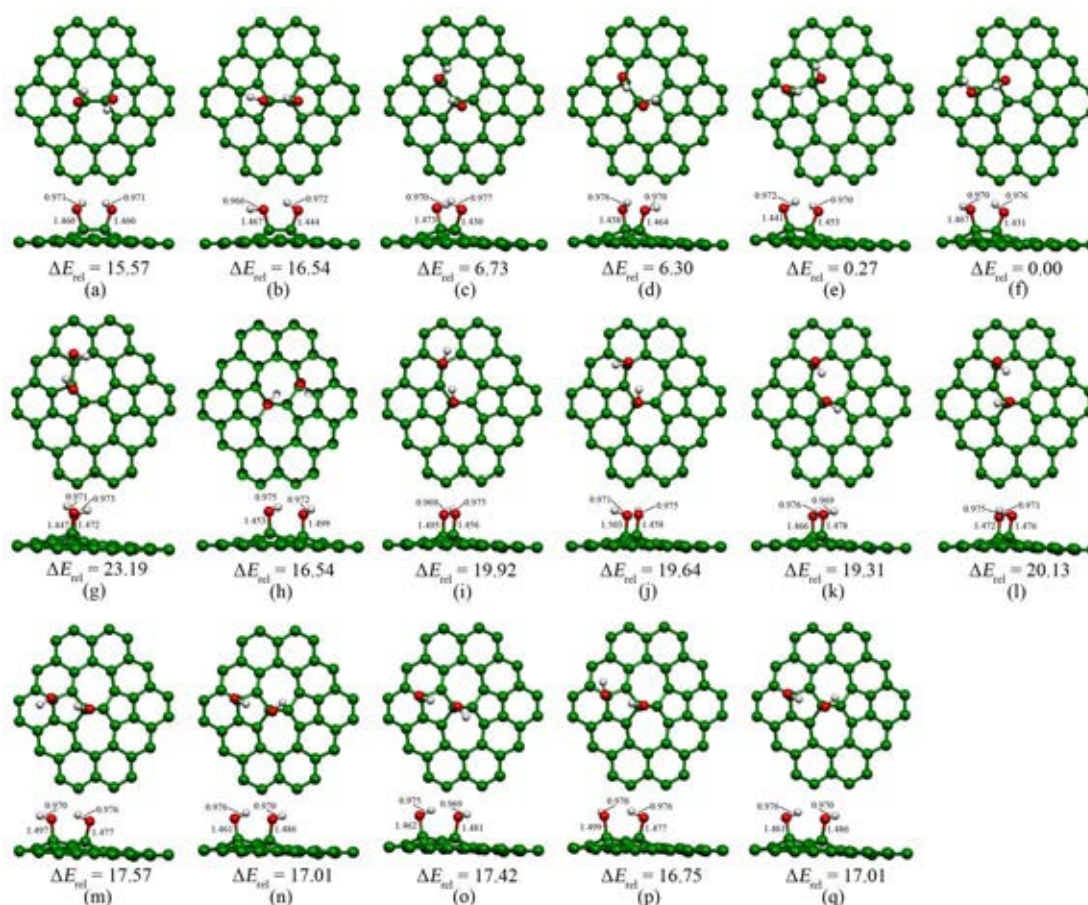


Figure 4.4 Configurations of di-hydroxide in vicinity of SW-defective graphene sheets, noted as (a) $(\text{OH})_2(1)/\text{GM3}$ (b) $(\text{OH})_2(2)/\text{GM3}$, (c) $(\text{OH})_2(3)/\text{GM3}$, (d) $(\text{OH})_2(4)/\text{GM3}$, (e) $(\text{OH})_2(5)/\text{GM3}$, (f) $(\text{OH})_2(6)/\text{GM3}$, (g) $(\text{OH})_2(7)/\text{GM3}$, (h) $(\text{OH})_2(8)/\text{GM3}$, (i) $(\text{OH})_2(9)/\text{GM3}$, (j) $(\text{OH})_2(10)/\text{GM3}$, (k) $(\text{OH})_2(11)/\text{GM3}$, (l) $(\text{OH})_2(12)/\text{GM3}$, (m) $(\text{OH})_2(13)/\text{GM3}$, (n) $(\text{OH})_2(14)/\text{GM3}$, (o) $(\text{OH})_2(15)/\text{GM3}$, (p) $(\text{OH})_2(16)/\text{GM3}$ and (q) $(\text{OH})_2(17)/\text{GM3}$. Their relative energies and bond lengths are in kcal/mol and Å, respectively. Their relative energies and bond lengths are in kcal/mol and Å, respectively.

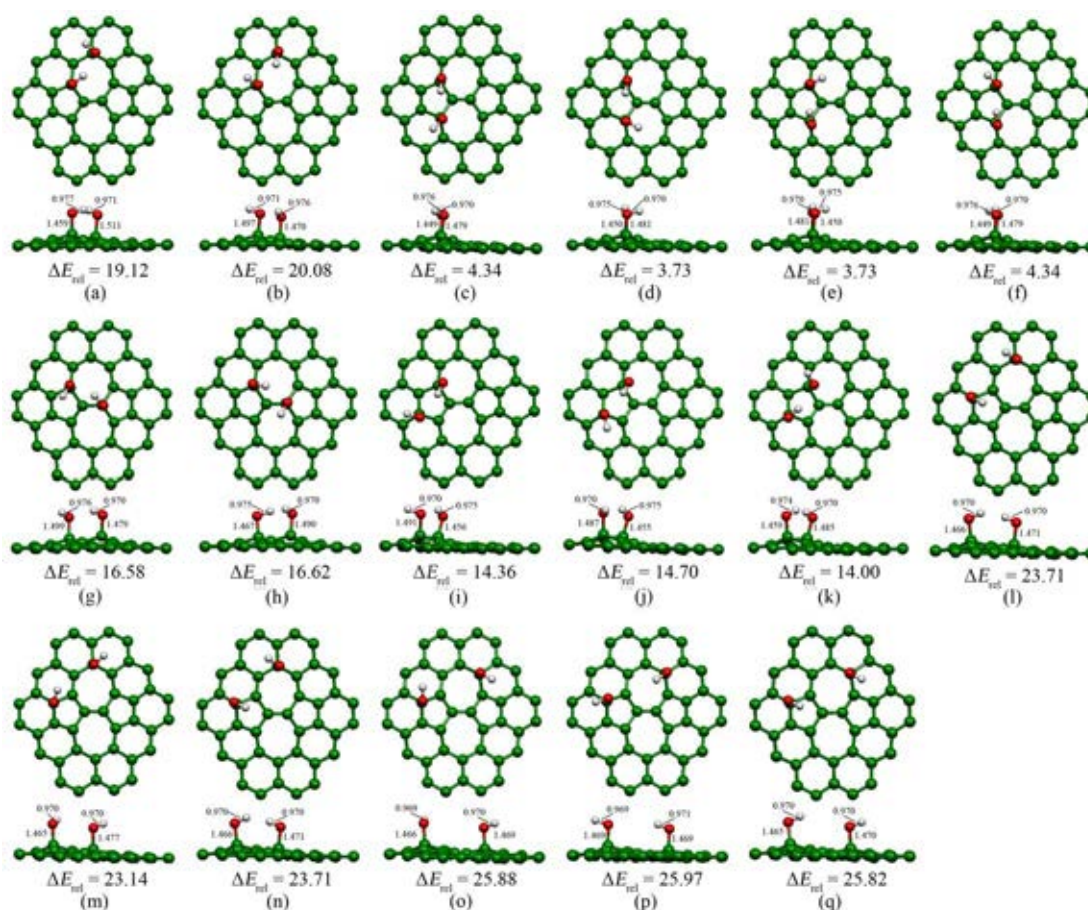


Figure 4.5. Configurations of di-hydroxide in vicinity of SW-defective graphene sheets, noted as (a) $(\text{OH})_2(18)/\text{GM3}$, (b) $(\text{OH})_2(19)/\text{GM3}$, (c) $(\text{OH})_2(20)/\text{GM3}$, (d) $(\text{OH})_2(21)/\text{GM3}$, (e) $(\text{OH})_2(22)/\text{GM3}$, (f) $(\text{OH})_2(23)/\text{GM3}$, (g) $(\text{OH})_2(24)/\text{GM3}$, (h) $(\text{OH})_2(25)/\text{GM3}$, (i) $(\text{OH})_2(26)/\text{GM3}$, (j) $(\text{OH})_2(27)/\text{GM3}$, (k) $(\text{OH})_2(28)/\text{GM3}$, (l) $(\text{OH})_2(29)/\text{GM3}$, (m) $(\text{OH})_2(30)/\text{GM3}$, (n) $(\text{OH})_2(31)/\text{GM3}$, (o) $(\text{OH})_2(32)/\text{GM3}$, (p) $(\text{OH})_2(33)/\text{GM3}$ and (q) $(\text{OH})_2(34)/\text{GM3}$. Their relative energies and bond lengths are in kcal/mol and Å, respectively. Their relative energies and bond lengths are in kcal/mol and Å, respectively.

4.3 Formations for carbonyl and carboxyl GOs

Optimized structures of carbonyl and carboxyl graphene oxide sheets are shown in Figure 4.6. Three types of carbonyl GOs, namely carbonyl locate at (i) armchair edge, (ii) zigzag edge connection with armchair edge and (iii) middle zigzag edge were found. Only one type of carboxyl GO of which carboxyl is located at the armchair edge. Reaction energies for oxidation processes of graphene sheets at their edges to afford carbonyl and carboxyl GOs are shown in Table 4.5. The reaction energies for oxidation of graphene by oxygen molecule to afford carbonyl GO and hydrogen molecule are within the range of -64.74 to -60.47 kcal/mol. The carboxylation as oxidation hydrogenation of graphene by hydrogen molecule to afford carboxyl GO and methane molecule, its reaction energy of -67.18 kcal/mol was found.

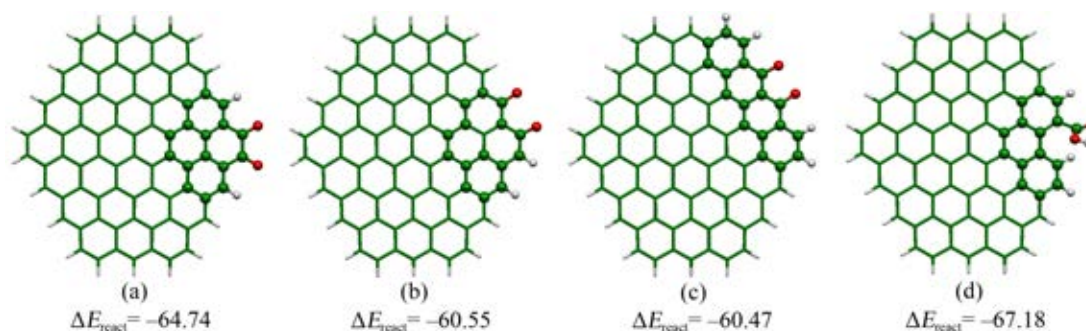


Figure 4.6 Optimized structures of carbonyl GOs of which oxygen atoms bonded to C atoms at (a) armchair edge, (b) at zigzag edge connection with armchair edge, (c) at middle zigzag edge and (d) carboxyl GO afforded due to carbon atom at armchair edge. Ball shaped atoms were treated as flexible atoms employed in structure optimizations. All the reaction energies (kcal/mol) for GOs are computed based on graphene Model 4, except reaction in (c) based on Model 5.

Table 4.5 Reaction energies for oxidation processes of graphene sheets at their edges to afford carbonyl and carboxyl GOs.

Oxidation	$\Delta E_{\text{react}}^{\text{a}}$
<i>Carbonylation:</i>	
$\text{C}_{80}\text{H}_{22}(1)^{\text{b}} + \text{O}_2 \rightarrow (\text{OC})_2\text{-C}_{78}\text{H}_{20}(1) + \text{H}_2$	-64.74
$\text{C}_{80}\text{H}_{22}(2)^{\text{b}} + \text{O}_2 \rightarrow (\text{OC})_2\text{-C}_{78}\text{H}_{20}(2) + \text{H}_2$	-60.55
$\text{C}_{80}\text{H}_{22}(3)^{\text{c}} + \text{O}_2 \rightarrow (\text{OC})_2\text{-C}_{78}\text{H}_{20}(3) + \text{H}_2$	-60.47
<i>Carboxylation:</i>	
$\text{C}_{80}\text{H}_{22}^{\text{b}} + \text{H}_2\text{O}_2 + \text{H}_2 \rightarrow \text{HOOC-C}_{79}\text{H}_{21} + \text{CH}_4$	-67.18

^a In kcal/mol.

^b Using Model 4.

^c Using Model 5.

4.4 GO simulation for adsorption of 3H₂O₂ and 3O₂ on graphenes

Formation energies for GO simulations by random adsorptions of 3H₂O₂ and 3O₂ on basal planes of one and both sides of pristine and SW-defective graphene sheets are shown in Table 4.6. The epoxide to hydroxyl ratio in GOs is exactly 1:1. Table 6 shows that SW-defective graphenes of which strain energies are much higher than pristine graphene, can form GO with very stable configuration. Adsorption of 3H₂O₂ and 3O₂ on both sides of either pristine or SW-defective graphenes are much stronger than on one side. The optimized structures of GOs which randomly adsorb 3O₂+3H₂O₂ on one and both sides of their basal planes are shown in Figure 4.7.

Table 4.6 GO simulations for random adsorptions of $3\text{H}_2\text{O}_2$ and 3O_2 on basal planes of one and both sides of pristine and SW-defective graphene sheets.

Oxidation	$\Delta E_{\text{form}}^{\text{a}}$	$\Delta E_{\text{strain}}^{\text{a}}$
<i>Pristine G:</i>		
$\text{G} (\text{C}_{80}\text{H}_{22})^{\text{b}} + 3 \text{H}_2\text{O}_2 + 3\text{O}_2 \rightarrow \text{GO}(\text{a})^{\text{d}}$	-208.01	309.50
$\text{G} (\text{C}_{80}\text{H}_{22})^{\text{b}} + 3 \text{H}_2\text{O}_2 + 3\text{O}_2 \rightarrow \text{GO}(\text{b})^{\text{d}}$	-305.08	304.17
<i>SW-defective G:</i>		
$\text{G} (\text{C}_{80}\text{H}_{22})^{\text{c}} + 3 \text{H}_2\text{O}_2 + 3\text{O}_2 \rightarrow \text{GO}(\text{c})^{\text{d}}$	-290.51	400.48
$\text{G} (\text{C}_{80}\text{H}_{22})^{\text{c}} + 3 \text{H}_2\text{O}_2 + 3\text{O}_2 \rightarrow \text{GO}(\text{d})^{\text{d}}$	-356.46	377.80

^a In kcal/mol.

^b Using Model 2.

^c Using Model 3.

^d GO(a), GO(b), GO(c) and GO(d) are defined as shown in Fig. 8(a), 8(b), 8(c) and 8(d), respectively.

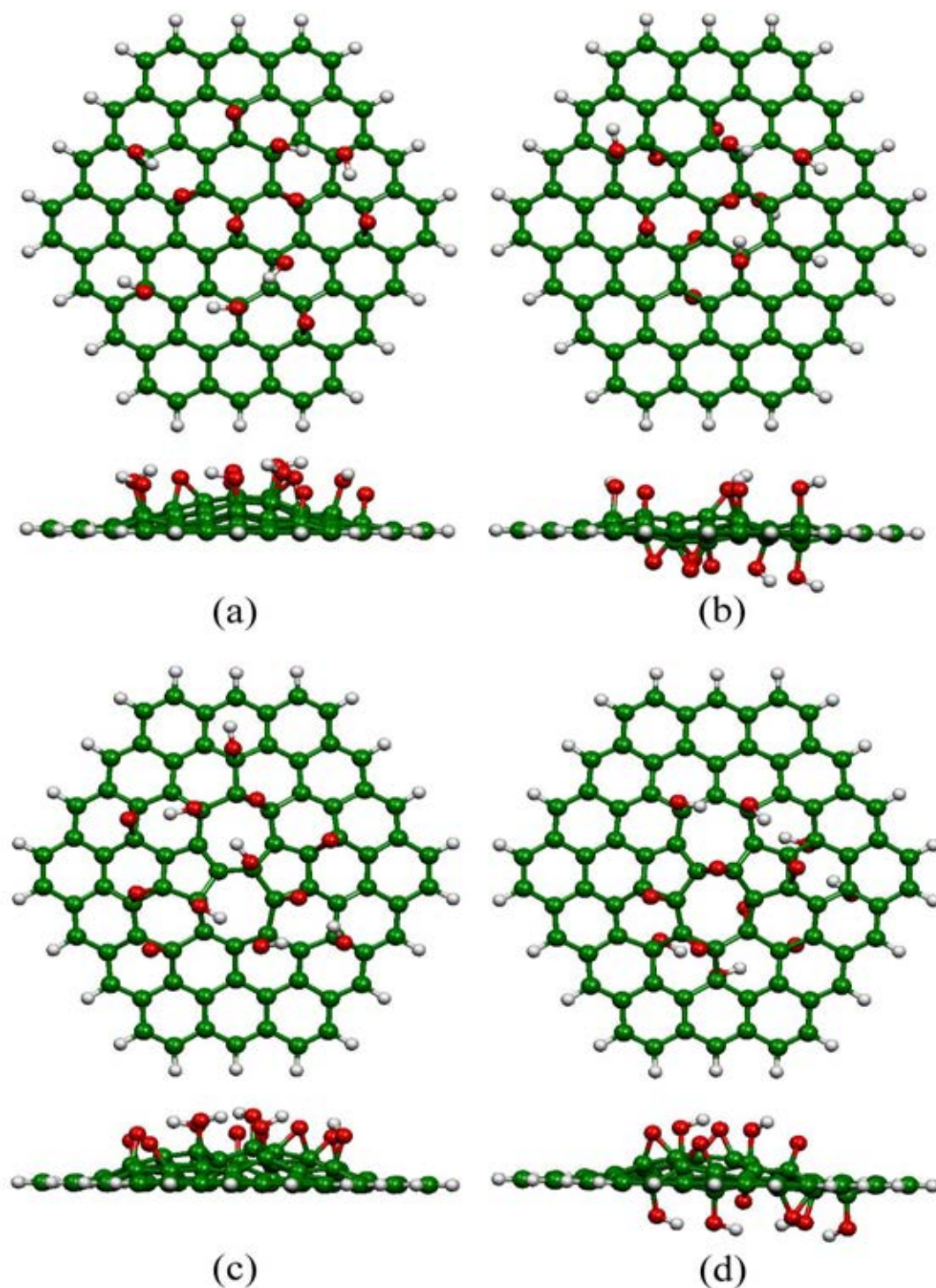


Figure 4.7 Optimized structures of GOs as random adsorptions of $3\text{O}_2+3\text{H}_2\text{O}_2$ on (a) one side, (b) both sides of pristine graphene sheets, (d) one side and (d) both sides of SW-defective graphene sheets. For adsorption on both sides, $\text{O}_2+2\text{H}_2\text{O}_2$ and $2\text{O}_2+\text{H}_2\text{O}_2$ are adsorbed on up and down sides, respectively. Top and side views are located at top and bottom, respectively.

CHAPTER V

5.1 Conclusions

Oxidation of pristine and SW-defective graphenes by oxygen and hydrogen peroxide to afford graphene oxides (GO) as epoxy and hydroxyl compounds were studied and their adsorption energies were obtained. The adsorption energies of oxygen on pristine and SW-defective graphenes as epoxy GOs are within the range of -22.43 to -1.52 and -42.39 to -24.82 kcal/mol, respectively. The adsorption energies of hydrogen peroxide on pristine and SW-defective graphenes as hydroxyl GOs are within the range of -47.55 to -30.742 and -78.80 to -46.58 kcal/mol, respectively. The adsorption abilities for the most stable GO configurations are in order: hydroxyl/SW-defective > hydroxyl/pristine (for hydrogen peroxide adsorption) > epoxy/SW-defective > epoxy/pristine (for oxygen molecule adsorption). Three types of carbonyl GOs, namely carbonyl locate at (i) armchair edge, (ii) zigzag edge connection with armchair edge and (iii) middle zigzag edge were found. The reaction energies for oxidation of graphene by oxygen molecule to afford carbonyl GO and hydrogen molecule are within the range of -64.74 to -60.47 kcal/mol. Only one type of carboxyl GO of which carboxyl is located at the armchair edge and its reaction energy is -67.18 kcal/mol. Formation energies for GO simulations by random adsorptions of $3\text{H}_2\text{O}_2$ and 3O_2 on basal planes of one and both sides of pristine and SW-defective graphene sheets are (-208.01 and -305.08 kcal/mol) and (-290.51 and -356.46 kcal/mol), respectively.

REFERENCES

- [1] Dikin, D.A., Stankovich, S., Zimney, E.J., Piner, R.D., Dommett, G.H.B., Evmenenko, G., Nguyen, S.T., and Ruoff, R.S. Preparation and characterization of graphene oxide paper. Nature 448 (2007): 457–60.
- [2] Burress, J.W., Gadipelli, S., Ford, J., Simmons, J.M., Zhou, W., and Yildirim, T. Graphene oxide frameworks materials: Theoretical predictions and experimental results. Angew. Chem. Int. Ed. 49 (2010): 8902–4.
- [3] Wu, X., Sprinkle, M., Li, X., Ming, F., Berger, C., and de Heer, W.A. Epitaxial–graphene/graphene-oxide junction: an essential step towards epitaxial graphene electronics. Phys. Rev. Lett. 101 (2008): 026801–4.
- [4] Kim, W.K., Jung, Y.M., Cho, J.H., Kang, J.Y., Oh, J.Y., Kang, H., Lee, H–J., Kim, J.H., Lee, S., Shin, H.J., Choi, J.Y., Lee, S.Y., Kim, Y.C., Han, I.T., Kim, J.M., Yook, J–G., Baik, S., and Jun, S.C. Radio–frequency characteristics of graphene oxide. Appl. Phys. Lett. 97 (2010): 193103–5.
- [5] Gao, Y., Yip, H–L., Chen, K–S., O’Malley, K.M., Acton, O., Sun, Y., Guy, T., Chen, H., and Jen, A.K–Y. Surface Doping of conjugated polymers by graphene oxide and its Application for organic electronic devices. Adv. Mater. 23 (2011): 1903–8.
- [6] Scheuermann, G.M., Rumi, L., Steurer, P., Bannwarth, W., and Mülhaupt, R. Palladium nanoparticles on graphite oxide and its functionalized graphene derivatives as highly active catalysts for the Suzuki–Miyaura coupling reaction. J. Am. Chem. Soc. 131 (2009): 8262–70.
- [7] Ng, Y.H., Iwase, A., Kudo, A., and Amal, R.J. Reducing graphene oxide on a visible–light BiVO₄ photocatalyst for an enhanced photoelectrochemical water splitting. J. Phys. Chem. Lett. 1 (2010): 2607–12.
- [8] Pyun, J. Graphene oxide as catalyst: Application of carbon materials beyond nanotechnology. Angew. Chem. Int. Ed. 50 (2011): 46–8.

- [9] Dhakshinamoorthy, A., Alvaro, M., Concepción, P., Fornés, V., and Garcia, H. Graphene oxide as an acid catalyst for the room temperature ring opening of epoxides. *Chem. Commun.* 48 (2012): 5443–5.
- [10] Dhakshinamoorthy, A., Alvaro, M., Puche, M., Fornés, V., and Garcia, H. Graphene oxide as catalyst for the acetalization of aldehydes at room temperature. *ChemCatChem* 4 (2012): 2026–30.
- [11] Psofogiannakis, G.M., and Froudakis, G.E. DFT study of hydrogen storage by spillover on graphite with oxygen surface groups. *J. Am. Chem. Soc.* 131 (2009): 15133–5.
- [12] Tylianakis, E., and Psofogiannakis, G.M., Li-doped pillared graphene oxide: a graphene-based nanostructured material for hydrogen storage. *J. Phys. Chem. Lett.* 1 (2010): 2459–64.
- [13] Chan, Y., and Hill, J.M. Hydrogen storage inside graphene-oxide frameworks, *Nanotechnology* 22 (2011): 305403–3.
- [14] Srinivas, G., Burrell, J., and Yildirim, T. Graphene oxide derived carbons (GODCs): synthesis and gas adsorption properties. *Energy Environ. Sci.* 5 (2012): 6453–9.
- [15] Chou, S.S., De, M., Luo, J., Rotello, V.M., and Huang, J. Nanoscale graphene oxide (nGO) as artificial receptors: implications for biomolecular interactions and sensing. *J. Am. Chem. Soc.* 134 (2012): 16725–33.
- [16] Hummers, W.S., and Offeman, R.E. Preparation of graphitic oxide. *J. Am. Chem. Soc.* 80 (1958): 1339–9.
- [17] Saxena, S., Tyson, T.A., and Negusse, E. Investigation of the local structure of graphene oxide. *J. Phys. Chem. Lett.* 1 (2010): 3433–37.
- [18] He, H., Klinowski, J., and Forster, M. A. Lerf, A new structural model for graphite oxide. *Chem. Phys. Lett.* 287 (1988): 53–6.
- [19] Dreyer, D.R., Park, S., Bielawski, C.W., and Ruoff, R.S. The chemistry of graphene oxide. *Chem. Soc. Rev.* 39 (2010): 228–40.
- [20] Hofmann, U., and Holst, R. Über die säurenatur und die methylierung von graphitoxyd. *Ber. Dtsch. Chem. Ges. B* 72 (1939): 754–71.
- [21] Ruess, G. Über das graphitoxhydroxyd (graphitoxyd). *Monatsh. Chem.* 76 (1946): 381–417.

- [22] Scholz, W., and Boehm, H.P.Z. Untersuchungen am graphitoxyd. Anor. Allg. Chem. 369 (1969): 327–340.
- [23] Nakajima, T., Mabuchi, A., and Hagiwara, R. A new structure model of graphite oxide. Carbon 26 (1988): 357–61.
- [24] Boukhvalov, D.W., and Katsnelson, M.I. Modeling of graphite oxide. J. Am. Chem. Soc. 130 (2008): 10697–701.
- [25] Lahaye, R.J.W.E., Jeong, H.K., Park, C.Y., and Lee, Y.H. Density functional theory study of graphite oxide for different oxidation levels. Phys. Rev. B 79 (12) (2009) 125435–43.
- [26] Yan, J.A., Xian, L., Chou, M.Y. Structural and electronic properties of oxidized graphene. Phys. Rev. Lett. 103 (2009): 086802–5.
- [27] Yan, J.A., and Chou, M.Y. Oxidation functional groups on graphene: Structural and electronic properties. Phys. Rev. B 82 (2010) : 125403–12.
- [28] Wang, L., Sun, Y.Y., Lee, K., West, D., Chen, Z.F., Zhao, J.J., and Zhang, S.B. Stability of graphene oxide phases from first-principles calculations. Phys. Rev. B 83 (2010): 161406–9.
- [29] Zhu, Y., Murali, S., Cai, W., Li, X., Suk, J., Potts, J.R., and Ruoff, R.S. Graphene and graphene oxide: Synthesis, properties, and application. Adv. Mater. 22 (2012): 3906–24.
- [30] Medhekar, N.V., Ramasubramaniam, A., Ruoff, R.S., Shenoy, V.B. Hydrogen bond networks in graphene oxide composite paper: Structure and mechanical properties. ACS Nano 4 (2010): 2300–6.
- [31] De La Cruz, A.F., and Cowley, J.M. Structure of graphitic oxide. Nature 196 (1962): 468–9.
- [32] He, H., Riedl, T., Lerf, A., and Klinowski, J. Solid-state NMR studies of the structure of graphite oxide. J. Phys. Chem. 100 (1996): 19954–8.
- [33] Lerf, A., He, H., Riedl, T., Forster, M., and Klinowski, J. ¹³C and ¹H MAS NMR studies of graphite oxide and its chemically modified derivatives. J. Solid State Ionics 10 (1997): 857–62.
- [34] He, H., Klinowski, J., Forster, M., Lerf, A. A new structural model for graphite oxide. Chem. Phys. Lett. 287 (1998): 53–6.

- [35] Lerf, A., He, H., Forster, M., and Klinowski, J. Structure of graphite oxide revisited. *J. Phys. Chem. B* 102 (1998): 4477–82.
- [36] Szabó, T., Berkesi, O., and Dékány, I. DRIFT study of deuterium-exchanged graphite oxide. *Carbon* 43 (2005): 3181–94.
- [37] Szabó, T., Tombácz, E., Illés, E., and Dékány, I. Enhanced acidity and pH-dependent surface charge characterization of successively oxidized graphite oxides. *Carbon* 44 (2006): 537–45.
- [38] Szabó, T., Berkesi, O., Forgó, P., Josepovits, K., Sanakis, Y., Petridis, D., and Dékány, I. Evolution of surface functional groups in a series of progressively oxidized graphite oxides. *Chem. Mater.* 18 (2006): 2740–9.
- [39] Cai, W., Piner, R.D., Stadermann, F.J., Park, S., Shaibat, M.A., Ishii, Y., Yang, D., Velamakanni, A., An, S.J., Stoller, M., An, J., Chen, D., and Ruoff, R.S. Synthesis and solid-state NMR structural characterization of ¹³C-labeled graphite oxide. *Science* 321 (2008): 1815–7.
- [40] Li, Z., Zhang, W., Luo, Y., Yang, J., and Hou, J.G. How graphene is cut upon oxidation? *J. Am. Chem. Soc.* 131 (2009): 6320–1.
- [41] Ghaderi, N., Peressi, M. First-principle study of hydroxyl functional groups on pristine, defected graphene, and graphene epoxide. *J. Phys. Chem. C* 114 (2010): 21625–30.
- [42] Hunt, A., Dikin, D.A., Kurmaev, E.Z., Boyko, T.D., Bazylewski, P., Chang, G.S., and Moewes, A. Epoxide speciation and functional group distribution in graphene oxide paper-like materials. *Adv. Funct. Mater.* 22 (2012): 3950–7.
- [43] Hontoria-Lucas, C., López-Peinado, A.j., López-Gozález, J.D.D., Roja-Cervantes, M.L., and Martín-Aranda, R.M. Study of oxygen containing groups in a series of graphite oxides: Physical and chemical characterization. *Carbon* 33 (1995): 1585–92.
- [44] Bourlinos, A.B., Gournis, D., Petridis, D., Szabo, T., Szeri, A., and Dekany, I. Graphite oxide: Chemical reduction to graphite and surface modification with primary aliphatic amines and Amino acids. *Langmuir* 19 (2003): 6050–5.

- [45] Worsley, K.M., Ramesh, P., Mandal, S.K., Nigogi, S., Itkis, M.E., and Haddon, R.C. Soluble graphene derived from graphite fluoride. Chem. Phys. Lett. 445 (2007): 51–6.
- [46] Mkhoyan, K.A., Contryman, A.W., Silcox, J., Stewart, D.A., Eda, G., Mattevi, C., Miller, S., and Chhowall, M. Atomic and electronic structure of graphene–oxide. Nano. Lett. 9 (2009): 1058–1063.
- [47] Zhang, T–Y., and Zhang, D. Aqueous colloids of graphene oxide nanosheets by exfoliation of graphite oxide without ultrasonication. Bull. Mater. Sci. 34 (2011): 25–28.
- [48] Lu, N., Yin, D., Li, Z., and Yang, J. Structural of graphene oxide; thermodynamics versus kinetic” J. Phys. Chem. C 115 (2011): 11991–5.
- [49] Levine, N. Quantum chemistry. 6th edition. Pearson prentice hall, 2010.
- [50] Engel, T., and Reid, P. Physical chemistry. Pearson benjamin chummings, 2009.
- [51] Atkins, P., and De Paula, J. Physical Chemistry. 8th edition. W. H. Freeman Company, 2006.
- [52] Mueller, M. Fundamental of Quantum Chemistry: Molecular Spectroscopy and Modern Electronic Structure Computations. New York: Kluwer Academic/Plenum Publishers, 2001.
- [53] Koch, W., and Holthausen, M.C. A Chemist’s Guide to Density Functional Theory. 2nd edition. Germany: Wiley–VCH, 2001.
- [54] Lowe, J.P., and Peterson, K.A. Quantum Chemistry. 3rd edition. London: Elsevier Academic Press, 2006.
- [55] Kohn, W., and Sham, L.J. Self–consistent equations including exchange and correlation effects. Phys. Rev. 140 (1965): 1133–8.
- [56] Lewars, E. Computational chemistry: Introduction to Theory and Applications of Molecular and Quantum Mechanics. 2nd edition. Canada: Springer, 2003.
- [57] Engel, E., and Dreizler, R.M. Density Functional Theory. London: Springer, 2011.
- [58] Cramer, C.J. Essentials of Computational Chemistry: Theory and Models. 2nd edition. Singapore: John Wiley and Sons, 2006.

- [59] Parr, R.G., and Yang, W. Density-Functional Theory of Atoms and Molecules. 1st edition. England: Oxford University Press Inc, 1994.
- [60] Beck, A.D. Density functional thermochemistry. III. The role of exact exchange. J. Chem. Phys. 98 (1993): 5648-52.
- [61] Beck, A.D. Density-functional exchange-energy approximation with correct asymptotic behavior. J. Chem. Phys. 104 (1996): 3100-3109.
- [62] Lee, C., Yang, W., and Parr, R.G. Development of the Colle-Salvetti correlation-energy formula into a functional of the electron density. Phys. Rev. B 37 (1988): 785-9.
- [63] Stewart J.J.P. Optimization of parameters for semi-empirical methods II. Applications. J. Comput. Chem. 10 (1989): 221-64.
- [64] Frisch, M.J., Trucks, G.W., Schlegel, H.B., Scuseria, G.E., Robb, M.A., Cheeseman, J.R., and et al. GUASSIAN 03, Revision D.02. Wallingford, Ct: Gaussian Inc., 2006.
- [65] Stone, A.J., and Wales, D.J. Theoretical studies of icosahedral C₆₀ and some related species Chem. Phys. Lett. 128 (1986): 501-3.

APPENDIX

APPENDIX A

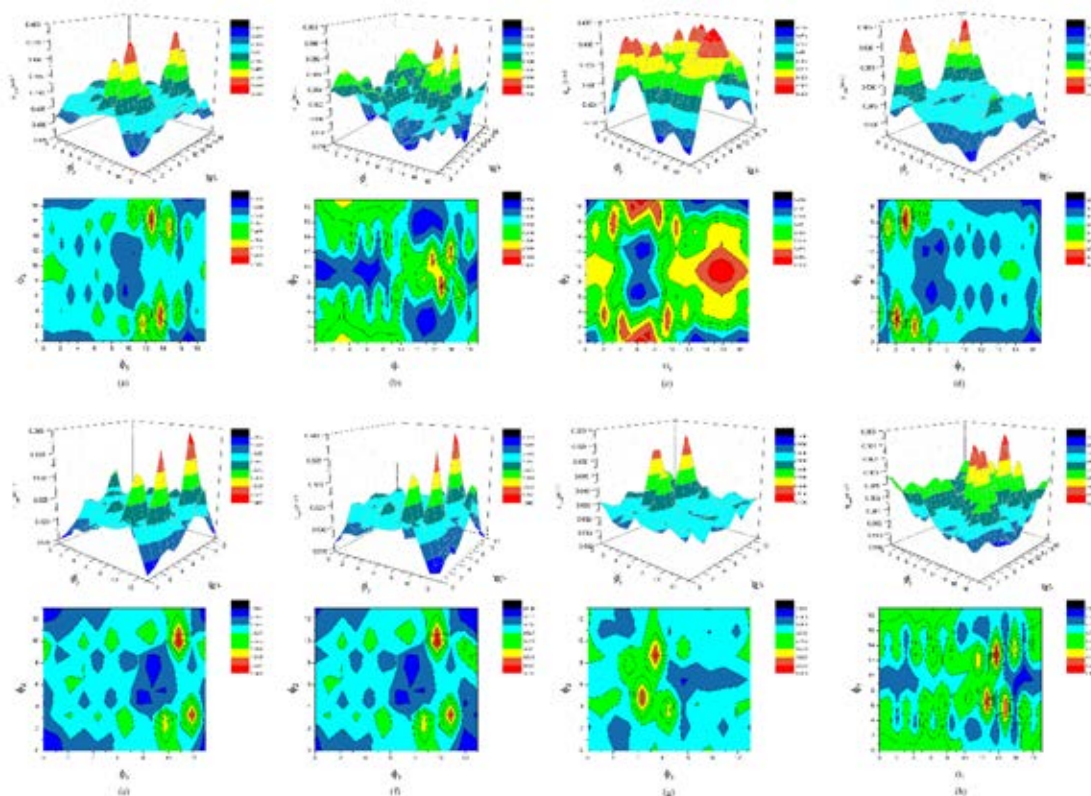


Figure A-1. 3D (top) and contour (bottom) plots for (a) scan #1, (b) scan #2, (c) scan #3, on SW-defect sheets (d) scan #4, (e) scan #5, (f) scan #6, (g) scan #7 and (h) scan #8, of which dihedral angles parameters for PES scan (φ_1 , φ_2) are defined in Figure A-3.

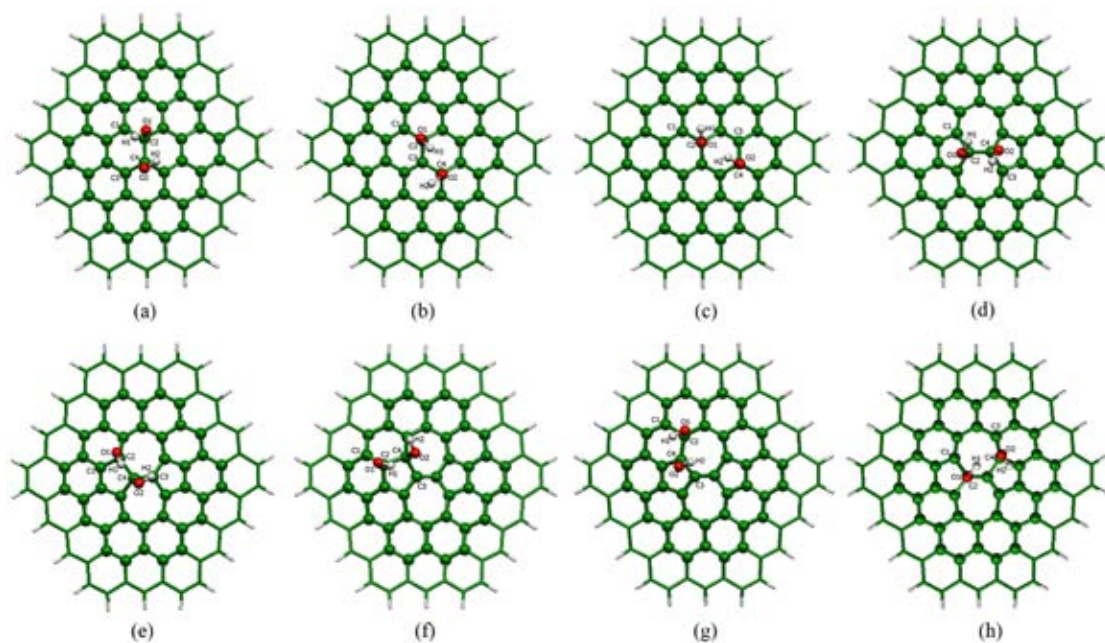


Figure A-2. Atomic numbering for double hydroxide located on pristine graphene sheets for (a) scan #1, (b) scan #2, (c) scan #3, on SW-defect sheets (d) scan #4, (e) scan #5, (f) scan #6, (g) scan #7 and (h) scan #8, of which dihedral angles parameters for PES scan are $(\varphi_1 = -178.8, \varphi_2 = -12.9)$, $(\varphi_1 = 0.0, \varphi_2 = 59.3)$, $(\varphi_1 = -180.0, \varphi_2 = -60.0)$, $(\varphi_1 = -180.0, \varphi_2 = 180.0)$, $(\varphi_1 = -180.0, \varphi_2 = -180.0)$, $(\varphi_1 = 0.0, \varphi_2 = 0.0)$, $(\varphi_1 = 0.0, \varphi_2 = 0.6)$ and $(\varphi_1 = 0.0, \varphi_2 = 0.0)$, respectively.

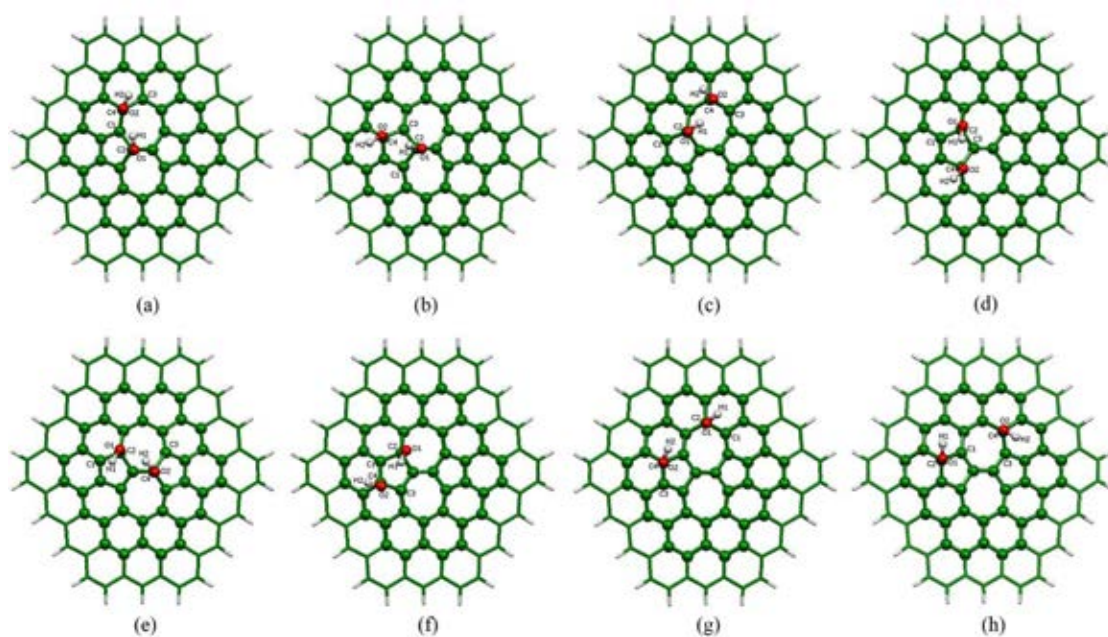


Figure A-3. Atomic numbering for double hydroxide located on SW-defect graphene sheets (a) for scan #9, (b) scan #10, (c) scan #11, (d) scan #12, (e) scan #13, (f) scan #14, (g) scan #15 and (h) scan #16, their dihedral angles parameters for PES scan are $(\varphi_1= 0.0, \varphi_2= 0.0)$, $(\varphi_1= -180.0, \varphi_2= 180.0)$, $(\varphi_1=0.0, \varphi_2= 0.0)$, $(\varphi_1= 0.0, \varphi_2= 0.0)$, $(\varphi_1= 0.0, \varphi_2= 0.0)$, $(\varphi_1= 0.0, \varphi_2= 0.0)$, $(\varphi_1= 0.0, \varphi_2= 0.0)$, $(\varphi_1= -0.5, \varphi_2= 115.5)$ and $(\varphi_1= 0.9, \varphi_2= 0.0)$, respectively.

Table A–1 Selected geometrical parameters for configurations of di-epoxide GOs.

Species	Bond distance ^a						Bond angle ^a				Dihedral angle ^b
	C1–O1	C2–O1	C1–C2	C3–O2	C4–O2	C3–C4	C1–C2–O1	C2–C1–O1	C3–C4–O2	C4–C3–O2	O1–C2–C3–O2
Model 1:											
O ¹ O ³ /GM1	1.460	1.433	1.497	1.433	1.460	1.497	59.7	58.0	58.0	59.7	0.0
O ¹ O ³ '/GM1	1.477	1.447	1.476	1.443	1.469	1.485	60.7	58.7	58.5	60.2	–61.9
O ¹ *O ¹ '/GM1	–	1.405	–	1.432	1.483	1.478	–	–	57.8	61.2	–
O ¹ O ³ /GM1	1.478	1.447	1.469	1.447	1.478	1.469	60.9	58.8	58.8	60.9	123.7
O ¹ *O ² /GM1	–	1.400	–	1.431	1.484	1.476	–	–	57.8	61.4	–
O ¹ O ³ '/GM1	1.488	1.442	1.472	1.439	1.478	1.480	61.4	58.3	58.3	60.8	–179.1
Model 3:											
O ² O ² '/GM3	1.478	1.443	1.497	1.443	1.478	1.497	60.4	58.0	58.0	60.4	0.0
O ² O ³ '/GM3	1.478	1.451	1.451	1.450	1.477	1.493	60.3	58.5	58.5	60.2	65.3
O ¹ O ³ /GM3	1.473	1.424	1.509	1.426	1.473	1.419	60.2	57.0	59.0	59.0	–4.6
O ¹ O ⁵ /GM3	1.477	1.426	1.504	1.453	1.464	1.501	60.5	57.2	58.7	59.4	60.5
O ⁶ O ² /GM3	1.461	1.456	1.457	1.427	1.469	1.423	60.2	59.9	59.1	62.1	–65.7
O ² O ³ '/GM3	1.457	1.442	1.488	1.438	1.461	1.534	59.6	58.6	57.3	58.8	–2.9
O ² O ² '/GM3	1.486	1.441	1.494	1.441	1.486	1.494	60.8	57.9	57.8	60.8	–113.6
O ⁶ O ⁵ /GM3	1.487	1.433	1.501	1.432	1.483	1.506	60.9	57.3	57.2	60.6	179.7
O ¹ O ³ /GM3	1.491	1.434	1.483	1.457	1.455	1.408	61.4	57.7	61.2	61.0	–128.5
O ¹ O ⁵ /GM3	1.470	1.439	1.494	1.453	1.476	1.489	60.1	58.1	58.7	60.2	177.6
O ⁶ O ³ /GM3	1.464	1.451	1.462	1.442	1.449	1.422	60.4	59.4	60.3	60.8	176.3
O ⁶ O ⁵ /GM3	1.478	1.454	1.459	1.449	1.510	1.481	61.0	59.4	57.9	62.0	124.8

^a In Å, ^b In degrees.

Table A–2 Selected geometrical parameters for configurations of di–hydroxyl GOs

Species	Bond distance ^a				Bond angle ^a		Dihedral angle ^b	
	C2–O1	O1–H1	C2–O2	O2–H2	θ_1	θ_2	ϕ_1	ϕ_2
Cluster Model 2								
(OH) ₂ (1)/GM2	1.450	0.968	1.450	0.968	105.9	105.9	–58.3	58.5
(OH) ₂ (2)/GM2	1.459	0.971	1.459	0.971	105.7	105.7	66.4	–177.1
(OH) ₂ (3)/GM2	1.475	0.977	1.515	0.971	104.9	105.9	166.6	69.2
(OH) ₂ (4)/GM2	1.474	0.977	1.511	0.970	105.3	106.7	159.3	–167.5
(OH) ₂ (5)/GM2	1.516	0.971	1.474	0.976	105.8	104.8	52.6	–46.3
(OH) ₂ (6)/GM2	1.511	0.970	1.472	0.977	106.8	105.3	–70.5	–39.6
(OH) ₂ (7)/GM2	1.495	0.970	1.461	0.977	106.7	105.3	–59.6	62.4
(OH) ₂ (8)/GM2	1.494	0.970	1.461	0.977	106.7	105.3	58.1	57.8
(OH) ₂ (9)/GM2	1.462	0.977	1.492	0.970	105.3	106.8	–177.5	–178.3
(OH) ₂ (10)/GM2	1.462	0.977	1.493	0.970	105.3	106.6	178.0	–62.8
Cluster Model 3								
(OH) ₂ (1)/GM3	1.460	0.971	1.460	0.971	105.4	105.4	–72.3	–72.3
(OH) ₂ (2)/GM3	1.444	0.972	1.467	0.966	105.7	107.9	–141.0	36.4
(OH) ₂ (3)/GM3	1.473	0.970	1.430	0.977	106.4	104.1	–156.7	148.5
(OH) ₂ (4)/GM3	1.438	0.976	1.464	0.970	104.7	106.4	91.84	34.24
(OH) ₂ (5)/GM3	1.441	0.972	1.453	0.970	104.8	106.3	–164.9	174.0
(OH) ₂ (6)/GM3	1.467	0.970	1.431	0.976	106.8	104.7	–34.0	–96.12
(OH) ₂ (7)/GM3	1.472	0.971	1.447	0.973	105.9	104.7	–167.1	176.8
(OH) ₂ (8)/GM3	1.453	0.975	1.499	0.972	104.5	106.1	–75.4	–156.4
(OH) ₂ (9)/GM3	1.456	0.975	1.495	0.969	106.2	107.7	–24.4	41.7
(OH) ₂ (10)/GM3	1.458	0.975	1.503	0.971	105.6	105.8	–36.0	164.9
(OH) ₂ (11)/GM3	1.478	0.969	1.466	0.976	106.6	106.0	–163.2	–93.5
(OH) ₂ (12)/GM3	1.476	0.971	1.472	0.975	106.4	105.4	63.7	–79.5
(OH) ₂ (13)/GM3	1.447	0.976	1.497	0.970	105.3	107.0	–69.9	–171.5
(OH) ₂ (14)/GM3	1.486	0.970	1.461	0.976	106.6	104.7	169.2	–48.3
(OH) ₂ (15)/GM3	1.481	0.969	1.462	0.975	106.8	105.2	70.6	–46.2
(OH) ₂ (16)/GM3	1.447	0.976	1.499	0.970	105.1	106.2	–66.1	74.9
(OH) ₂ (17)/GM3	1.486	0.970	1.461	0.976	106.6	104.7	169.0	–48.3
(OH) ₂ (18)/GM3	1.459	0.977	1.511	0.971	105.1	106.0	–165.2	165.8
(OH) ₂ (19)/GM3	1.497	0.971	1.470	0.976	106.0	105.4	–56.1	–75.1
(OH) ₂ (20)/GM3	1.479	0.970	1.449	0.976	107.2	105.7	64.4	168.3
(OH) ₂ (21)/GM3	1.481	0.970	1.450	0.975	106.6	105.6	59.5	–79.3
(OH) ₂ (22)/GM3	1.450	0.975	1.481	0.970	105.6	106.6	–177.7	45.8
(OH) ₂ (23)/GM3	1.449	0.976	1.479	0.970	105.7	107.2	–65.4	40.9
(OH) ₂ (24)/GM3	1.499	0.972	1.453	0.975	106.1	104.5	38.5	75.3
(OH) ₂ (25)/GM3	1.467	0.975	1.490	0.970	105.7	105.7	150.4	–176.5
(OH) ₂ (26)/GM3	1.456	0.975	1.491	0.970	105.5	106.5	41.2	–176.9
(OH) ₂ (27)/GM3	1.455	0.975	1.487	0.970	105.8	107.1	36.4	–59.4
(OH) ₂ (28)/GM3	1.485	0.970	1.459	0.974	106.2	104.5	–77.2	64.1
(OH) ₂ (29)/GM3	1.466	0.970	1.471	0.970	106.5	106.9	64.6	174.1
(OH) ₂ (30)/GM3	1.465	0.970	1.477	0.970	106.3	107.1	160.2	69.3
(OH) ₂ (31)/GM3	1.466	0.970	1.471	0.970	106.5	106.9	64.5	174.2
(OH) ₂ (32)/GM3	1.469	0.970	1.466	0.969	106.5	106.7	67.6	51.6
(OH) ₂ (33)/GM3	1.469	0.971	1.469	0.969	106.6	106.7	177.0	–63.0
(OH) ₂ (34)/GM3	1.470	0.970	1.465	0.970	106.4	106.7	–50.3	56.0

^a In Å, ^b In degrees.

VITAE

Name: Miss WIPARAT HOTARAT

Date of Birth: April 13rd, 1986

Place of Birth: Nongkhai, Thailand

Address: 1 Banduea T.Banduea A.Mueng, Nongkhai 43000, Thailand

Telephone: 089-9681397

E-mail address: h.wiparat@gmail.com

Educations:

2011-2013 M.Sc. (Physical Chemistry), Chulalongkorn University, Thailand

2005-2010 B.Sc. (Chemistry), Silpakorn University, Thailand

2001-2004 Pathumthep Witthayakarn high school, Nongkhai, Thailand

1998-2000 Pathumthep Witthayakarn secondary school, Nongkhai, Thailand

1992-1997 Ban Duea primary school, Nongkhai, Thailand

Publication: